AD-A265 311

CUMENTATION PAGE

Form Approved OMB No. 0704-0188

2

	2. REPORT DATE	3. REPORT TYPE AND DATES COVERED FINAL/01 SEP 91 TO 31 DEC 92

4. TITLE AND SUBTITLE "A SIMPLE MODEL OF MELT FRACTURE" (U)	5. FUNDING NUMBERS 2304/A1 AFOSR-91-0352
6. AUTHOR(S) Professor James Greenberg	
7. PERFORMING ORGANIZATION NAME(S) AND ADDRESS(ES) University of Maryland Dept of Math & Statistics Baltimore, MD 21228	8. PERFORMING ORGANIZATION REPORT NUMBER AEOSR-TR- 93 0323
9. SPONSORING/MONITORING AGENCY NAME(S) AND ADDRESS(ES) AFOSR/NM 110 DUNCAN AVE, SUTE B115 BOLLING AFB DC 20332-0001	10. SPONSORING/MONITORING AGENCY REPORT NUMBER AFOSR-91-0352
11. SUPPLEMENTARY NOTES	
12a. DISTRIBUTION/AVAILABILITY STATEMENT APPROVED FOR PUBLIC RELEASE: DISTRIBUTION IS UNLIMITED	12b. DISTRIBUTION CODE UL

DTIC ELECTE JUN 02 1993 S E D

13. ABSTRACT (Maximum 200 words)

The PI produced an excellent explanation of the unpleasant shark-skinning observed in certain polymer extrusion processes. This work has been brought to the attention of researchers at Corning and Hoechst Celanese and Greenberg and Demay will work this summer with members of the Materials Sciences Center at the Ecole Nationale Superieure des Mines de Paris led by J.F. Agassant. One goal of this work is to see if the same oscillatory phenomena is present when one replaces the slip boundary condition by a no slip one and looks instead at materials whose shear stress - strain rate constitutive equation has a spinodal type nonlinearity. A difficult question also worth pursuing is whether now understanding the nature of the flow instability - a switch from a slip to a no slip boundary condition at the wall of the capillary tube - if it is possible to control the inlet flow to the capillary in the unstable regime in such a way as to reduce the oscillations and shark skinning of the final product.

14. SUBJECT TERMS 93 020	15. NUMBER OF PAGES 58
	16. PRICE CODE

17. SECURITY CLASSIFICATION OF REPORT	18. SECURITY CLASSIFICATION OF THIS PAGE	19. SECURITY CLASSIFICATION OF ABSTRACT	20. LIMITATION OF ABSTRACT
UNCLASSIFIED	UNCLASSIFIED	UNCLASSIFIED	SAR(SAME AS REPORT)

NSN 7540-01-280-5500

Standard Form 298 (Rev 2-89)
Prescribed by ANSI Std Z39-18
298-102

93-12312

Final Technical Report on the Research based on the proposal AFOSR-91-0352 for the period September 1, 1991 through December 31, 1992.

The original proposal was to support two months of Greenberg's research efforts on Lattice Gases and Transport Processes while he was on sabbatical leave in Europe from the period January 1, 1992 through December 31, 1992. Before leaving for Europe,Greenberg contacted his program officer, Dr. Arje Nachman, and requested a change in the scope of the project. Greenberg proposed to work instead on problems in Plastic Flow and Oscillatory Flows in Molten Polymers. Dr. Nachman approved this request.

During the period June 1, 1992 through September 30, 1992 Greenberg was resident at the University of Nice and worked with Yves Demay and Anne Nouri on the revised research program. Two papers resulted from this effort:

(1) with Anne Nouri, Antiplane Shearing Motions of a Visco-Plastic Solid; to appear in SIAM J. Math. Analysis

(2) with Y. Demay, A Simple Model of Melt Fracture, to appear in European Journal of Applied Mathematics.

The latter paper nicely compliments work of Greg Forest, also supported in Dr. Nachman's program, and gives an excellent explanation of the unpleasant shark-skinning observed in certain polymer extrusion processes. This work has been brought to the attention of researchers at Corning and Hoechst Celanese and Greenberg and Demay will work this summer with members of the Materials Sciences Center at the Ecole Nationale Superieure des Mines de Paris led by J. F. Agassant. One goal of this work is to see if the same oscillatory phenomena is present when one replaces the slip boundary condition by a no slip one and looks instead at materials whose shear stress - strain rate constitutive equation has a spinodal type nonlinearity. A difficult question also worth pursuing is whether now understanding the nature of the flow instability - a switch from a slip to a no slip boundary condition at the wall of the capillary tube - if it is possible to control the inlet flow to the capillary in the unstable regime in such a way as to reduce the oscillations and shark skinning of the final product.

DTIC QUALITY INSPECTED 2

A Simple Model of Melt Fracture

J. M. Greenberg*
Department of Mathematics and Statistics
University of Maryland, Baltimore County
Baltimore, MD 21228

Y. Demay
Institut Non-Linéaire de Nice
U.M.R.-C.N.R.S. no19
Université de Nice
Parc Valrose, 06034 Nice (France)

1. Model Development

A classical measure of viscosity of a molten polymer is obtained by studying the relationship between the flow rate and pressure drop when the polymer is flowing in a capillary tube of radius R and length L. For a linearly viscous polymer with viscosity η_1 this relationship takes the form:

$$\bar{w} = \frac{R^2}{8\eta_1}\frac{\Delta P}{L} \tag{1.1}$$

where ΔP is the pressure drop across the capillary from $z = 0$ to $z = L$ and $\bar{w}$ is the mean velocity taken over a cross-section perpendicular to the flow direction. For such a flow, the wall shear is given by

$$\tau_w = -\frac{R\Delta P}{2L} \tag{1.2}$$

*This research was partially supported by the U.S. National Science Foundation, the U.S. Department of Energy and U.S. Air Force Office of Scientific Research.

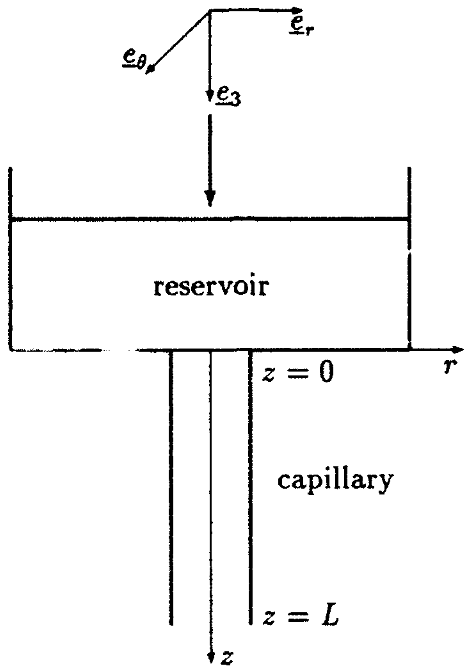

Figure 1.

and thus (1.1) is equivalent to the following relationship between $\bar{w}$ and τ_w:

$$\bar{w} = -\frac{R}{4\eta_1}\tau_w. \tag{1.3}$$

These relationships follow from the local equilibrium equations for a linearly viscous fluid subjected to a constant pressure gradient and a no slip boundary condition at the capillary wall. The underlying flow in this case is Poiseuille. If the no slip boundary condition is replaced by the slip boundary condition

$$w(R) = -\frac{R(4F-1)}{4\eta_1}\tau_w, \quad F \geq \frac{1}{4}, \tag{1.4}$$

then the relation (1.2) still obtains but (1.1) is replaced by

$$\bar{w} = -\frac{R^2 F \Delta P}{2\eta_1 L} \tag{1.5}$$

or equivalently

$$\bar{w} = -\frac{RF}{\eta_1}\tau_w.^1 \tag{1.6}$$

[1]These relations are derived later in this section; for details see (1.27)–(1.32).

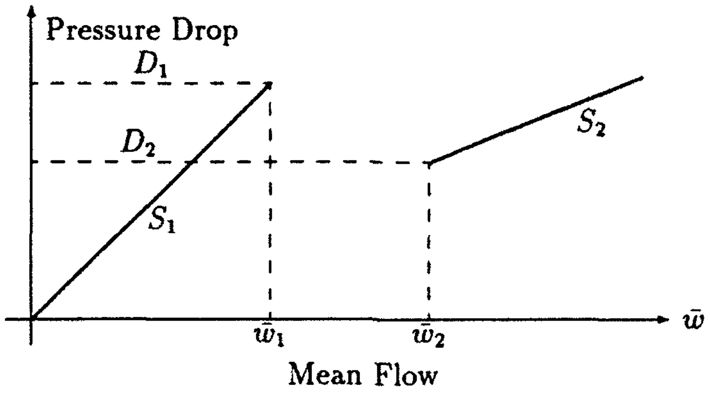

Figure 2.

For molten polymers one typically observes two distinctly different stable steady flow regimes (see Figure 2). For mean velocities $\bar{w} \leq \bar{w}_1$ one operates on the curve S_1 whereas for mean velocities $\bar{w} \geq \bar{w}_2$ one operates on the curve S_2. Experimental evidence indicates that the pressure drop D_1 associated with the velocity $\bar{w}_1$ is larger than the drop D_2 associated with $\bar{w}_2$. In general *one finds no stable steady flows with* velocities between $\bar{w}_1$ and $\bar{w}_2$; rather one observes oscillatory flows with mean velocities in the range $(\bar{w}_1, \bar{w}_2)$ and pressure drops in the range (D_2, D_1). One normally interprets such data as follows: on the curve S_1 the polymer satisfies a no slip boundary condition at the capillary wall whereas on the curve S_2 slipping at the wall is taking place. In general, the curves S_1 and S_2 are nonlinear which indicates that the polymer is not a simple linearly viscous fluid and that the slip boundary condition is really modeled by a nonlinear relationship between $w(R)$ and τ_w. These details will not concern us here. Our goal is a simple model which explains the gross features of the transition from steady to oscillatory flows.

Motivated by (1.3) and (1.6) we assume that $\bar{w}$ and τ_w are related by

$$\bar{w} = -\frac{RF}{\eta_1}\tau_w \tag{1.7}$$

where η_1 is the viscosity of the polymer, R is the radius of the capillary, and F is a dimensionless parameter which ranges between $1/4$ and $F_2 > 1/4$. Bearing in mind the relationship (1.2), we assume the existence of a switch curve (scaled as shown)

$$S(\bar{w}) = \begin{cases} \frac{D_1 R}{2L}, & \bar{w} < \frac{R^2 D_1}{8\eta_1 L} \\ \frac{D_1 R}{2L} + \frac{R}{2L}\left(\frac{D_2 - D_1}{\frac{R^2 F_2 D_2}{2\eta_1 L} - \frac{R^2 D_1}{8\eta_1 L}}\right)\left(\bar{w} - \frac{R^2 D_1}{8\eta_1 L}\right), & \frac{R^2 D_1}{8\eta_1 L} \leq \bar{w} \leq \frac{R^2 F_2 D_2}{2\eta_1 L} \\ \frac{D_2 R}{2L}, & \frac{R^2 F_2 D_2}{2\eta_1 L} < \bar{w} \end{cases} \tag{1.8}$$

which determines the stability of the curves S_1 and S_2; specifically we assume that F switches from $1/4$ to F_2 via the transition rule

$$T_0\frac{dF}{dt}=\begin{cases} F_2-F; & |\tau_w|>S(\bar{w})=S(F|\tau_w|) \\ \frac{1}{4}-F; & |\tau_w|<S(\bar{w})=S(F|\tau_w|)\end{cases} \tag{1.9}$$

where T_0 is a fixed relaxation time (see Figure 3).

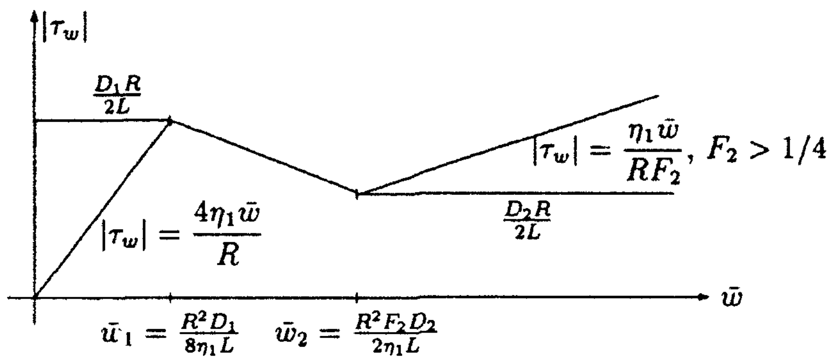

Figure 3.

Equation (1.7)–(1.9) are constitutive equations relating $\bar{w}$, F, and τ_w and these hold at each point z along the capillary. To these we must adjoin variants of the continuity and balance of momentum equations together with an equation of state relating the density to the pressure in the polymer. Again, the geometry of our system is shown in Figure 1 and our model accounts for what happens in the capillary tube, not the reservoir.

We assume the flow in the capillary is axisymmetric and that all quantities depend only on r, z, and t. We let ρ denote the polymer density, p denote the pressure, and assume that the velocity field $\underset{\sim}{u}$ and Cauchy stress tensor σ are of the form:

$$\underset{\sim}{u}=u\underline{e}_r+w\underline{e}_3 \tag{1.10}$$

and

$$\sigma=-p(\underline{e}_r\oplus\underline{e}_r+\underline{e}_\theta\oplus\underline{e}_\theta+\underline{e}_3\oplus\underline{e}_3)+\sigma^v_{rr}\underline{e}_r\oplus\underline{e}_r+\sigma^v_{\theta\theta}\underline{e}_\theta\oplus\underline{e}_\theta + \sigma^v_{33}\underline{e}_3\oplus\underline{e}_3+\tau(\underline{e}_3\oplus\underline{e}_r+\underline{e}_r\oplus\underline{e}_3).^2 \tag{1.11}$$

[2] $\underline{e}_r=(\cos\theta,\sin\theta,0)$, $\underline{e}_\theta=(-\sin\theta,\cos\theta,0)$, and for any vectors $\underline{a}=(a_1,a_2,a_3)$ and $\underline{b}=(b_1,b_2,b_3)$ we let $\underline{a}\oplus\underline{b}=\underline{a}^T\underline{b}$ where $\underline{a}^T=\begin{pmatrix}a_1\\a_2\\a_3\end{pmatrix}$.

$(\sigma^v_{rr}, \sigma^v_{\theta\theta}, \sigma^v_{33}, \tau)$ are the nonzero components of the viscous stress tensor and are assumed related to u and w by

$$(1.12)\qquad \begin{cases} \sigma^v_{rr} = \lambda_1(\frac{1}{r}\frac{\partial}{\partial r}(ru) + \frac{\partial w}{\partial z}) + 2\eta_1\frac{\partial u}{\partial r} \\ \sigma^v_{\theta\theta} = \lambda_1(\frac{1}{r}\frac{\partial}{\partial r}(ru) + \frac{\partial w}{\partial z}) + 2\eta_1\frac{u}{r} \\ \sigma^v_{33} = \lambda_1(\frac{1}{r}\frac{\partial}{\partial r}(r\frac{\partial u}{\partial r}) + \frac{\partial w}{\partial z}) + 2\eta_1\frac{\partial w}{\partial z} \\ \tau = \eta_1(\frac{\partial w}{\partial r} + \frac{\partial u}{\partial z}). \end{cases}$$

We do not make the Stokean hypothesis $3\lambda_1 + 2\eta_1 = 0$ but we do assume that $\lambda_1 = O(\eta_1)$. The governing equations are the continuity equation and balance of momentum in the directions $\underline{e}_r$, $\underline{e}_\theta$, and $\underline{e}_3$. These take the form

$$\text{(C)}\qquad \frac{\partial \rho}{\partial t} + \frac{1}{r}\frac{\partial}{\partial r}(r\rho u) + \frac{\partial}{\partial z}(\rho w) = 0,$$

$$(\text{M}_r)\qquad \frac{\partial}{\partial t}(\rho u) + \frac{1}{r}\frac{\partial}{\partial r}(r\rho u^2) + \frac{\partial}{\partial z}(\rho u w) - \frac{\partial p}{\partial r} + \frac{\partial \sigma^v_{rr}}{\partial r} + \frac{(\sigma^v_{rr} - \sigma^v_{\theta\theta})}{r} + \frac{\partial \tau}{\partial z} = 0,$$

$$(\text{M}_\theta)\qquad -\frac{1}{r}\frac{\partial p}{\partial \theta} = 0,$$

and

$$(\text{M}_3)\qquad \frac{\partial}{\partial t}(\rho w) + \frac{1}{r}\frac{\partial}{\partial r}(r\rho u w) + \frac{\partial}{\partial z}(\rho w^2) - \frac{\partial p}{\partial z} + \frac{\partial \sigma^v_{33}}{\partial z} + \frac{1}{r}\frac{\partial}{\partial r}(r\tau) = \rho g.$$

At the boundary, $r = R$, we assume that

$$\text{(BC)}\qquad u(R,z,t) = 0 \quad\text{and}\quad w(R,z,t) = -\frac{R}{4\eta_1}(4F-1)\tau_w(z,t),$$

where $F \geq 1/4$ is a dimensionless quantity depending on z and t and $\tau_w(z,t) = \tau(R,z,t)$ is the wall shear. In order that the stresses σ^v_{rr}, $\sigma^v_{\theta\theta}$, and σ^v_{33} be finite at $r = 0$, we also require that the radial component of the flow, u, vanishes faster than r as r tends to zero. To close the system we assume that the polymer is slightly compressible and that the following equation of state holds between the density and pressure:

$$\text{(EOS)}\qquad \rho = \rho_0\left(1 + \frac{\epsilon_1 p}{p_0}\right).$$

Here, ρ_0 and p_0 are reference values of the density and pressure and $0 < \epsilon_1 \ll 1$ is a dimensionless small parameter.

To assess which terms in this system are important and which may be neglected we cast the system in dimensionless form. We let

$$(1.13)\qquad r = Rr_1,\ z = Lz_1,\ \text{ and }\ t = \frac{2\epsilon_1\eta_1 L^2}{p_0 R^2}t_1$$

and

$$(1.14)\quad \begin{cases} \rho = \rho_0\rho_1,\ w = \frac{p_0R^2}{\eta_1 L}w_1,\ u = \frac{p_0R^3}{\eta_1 L^2}u_1,\ p = 2p_0p_1, \\ \tau = \frac{p_0R\tau^1}{L},\ \sigma^v_{rr} = p_0\left(\frac{R}{L}\right)^2\sigma^1_{r_1r_1},\ \sigma^v_{\theta\theta} = p_0\left(\frac{R}{L}\right)^2\sigma^1_{\theta\theta}, \\ \sigma^v_{33} = p_0\left(\frac{R}{L}\right)^2\sigma^1_{33},\ \text{ and }\ \tau_w = \frac{p_0R}{L}\tau^1_w. \end{cases}$$

Then it is a relatively easy calculation to show that (1.12) transforms to

$$(1.15)\quad \begin{cases} \sigma^1_{r_1r_1} = \mu\left(\frac{1}{r_1}\frac{\partial}{\partial r_1}(r_1u_1) + \frac{\partial w_1}{\partial z_1}\right) + 2\frac{\partial u_1}{\partial r_1} \\ \sigma^1_{\theta\theta} = \mu\left(\frac{1}{r_1}\frac{\partial}{\partial r_1}(r_1u_1) + \frac{\partial w_1}{\partial z_1}\right) + 2\frac{u_1}{r_1} \\ \sigma^1_{33} = \mu\left(\frac{1}{r_1}\frac{\partial}{\partial r_1}(r_1u_1) + \frac{\partial w_1}{\partial z_1}\right) + 2\frac{\partial w_1}{\partial z_1} \\ \tau^1 = \left(\frac{\partial w_1}{\partial r_1} + \epsilon_2\frac{\partial u_1}{\partial z_1}\right) \end{cases}$$

where

$$(1.16)\quad \mu = \frac{\lambda_1}{\eta_1} = O(1) \ \text{ and } \ \epsilon_2 = \frac{R}{L} \ll 1$$

and the equation of state becomes

$$(1.17)\quad \rho_1 = (1 + 2\epsilon_1 p_1).$$

The continuity equation transforms to

$$(1.18)\quad \frac{1}{2\epsilon_1}\frac{\partial \rho_1}{\partial t_1} + \frac{1}{r_1}\frac{\partial}{\partial r_1}(r_1\rho_1u_1) + \frac{\partial}{\partial z_1}(\rho_1 w_1) = 0$$

and (1.18), when combined with (1.17), yields

$$(1.19)\quad \frac{\partial p_1}{\partial t_1} + \frac{1}{r_1}\frac{\partial(r_1u_1)}{\partial r_1} + \frac{\partial w_1}{\partial z_1} + 2\epsilon_1\left(\frac{1}{r_1}\frac{\partial(r_1p_1u_1)}{\partial r_1} + \frac{\partial(p_1w_1)}{\partial z_1}\right) = 0.$$

Finally the three balance laws (M_r), (M_θ), and (M_3) take the form

$$(1.20)\quad \begin{aligned} &\frac{\epsilon_2^4\epsilon_3}{2\epsilon_1}\frac{\partial(\rho_1u_1)}{\partial t_1} + \frac{\epsilon_2^4\epsilon_3}{r_1}\frac{\partial}{\partial r_1}(r_1\rho_1u_1^2) + \epsilon_2^4\epsilon_3\frac{\partial(\rho_1u_1w_1)}{\partial z_1} \\ &\quad + \epsilon_2^3\left(\frac{(\sigma^1_{r_1r_1} - \sigma^1_{\theta\theta})}{r_1} + \frac{\partial\sigma^1_{r_1r_1}}{\partial r_1}\right) + \epsilon_2^2\frac{\partial\tau^1}{\partial z_1} = 2\frac{\partial p_1}{\partial r_1}, \end{aligned}$$

$$(1.21)\quad \frac{1}{r_1}\frac{\partial p_1}{\partial\theta} = 0,$$

and

$$(1.22)\quad \begin{aligned} &\frac{\epsilon_2^2\epsilon_3}{2\epsilon_1}\frac{\partial(\rho_1w_1)}{\partial t_1} + \epsilon_2^2\epsilon_3\left(\frac{1}{r_1}\frac{\partial(r_1\rho_1u_1w_1)}{\partial r_1} + \frac{\partial(\rho_1w_1^2)}{\partial z_1}\right) \\ &\quad + \epsilon_2^2\frac{\partial\sigma^1_{33}}{\partial z_1} - \epsilon_4(1 + 2\epsilon_1p_1) = 2\frac{\partial p_1}{\partial z_1} - \frac{1}{r_1}\frac{\partial(r_1\tau^1)}{\partial r_1} \end{aligned}$$

where ϵ_1 is the small parameter in (EOS), $\epsilon_2 = \frac{R}{L} \ll 1$ and

(1.23) $$\epsilon_3 \stackrel{\text{def}}{=} \frac{\rho_0 p_0 R^2}{\eta_1^2} \quad \text{and} \quad \epsilon_4 = \frac{\rho_0 g L}{p_0}.$$

Our principal simplification comes from assuming that $\frac{\epsilon_2^2 \epsilon_3}{\epsilon_1}$ and ϵ_4 are small and from neglecting all terms with ϵ's in (1.19)–(1.22). This leads us to the following reduced system

(1.24) $$\frac{\partial p_1}{\partial t_1} + \frac{1}{r_1}\frac{\partial (r_1 u_1)}{\partial r_1} + \frac{\partial w_1}{\partial z_1} = 0,$$

(1.25) $$\frac{\partial p_1}{\partial r_1} = \frac{\partial p_1}{\partial \theta} = 0,$$

and

(1.26) $$\frac{1}{r_1}\frac{\partial (r_1 \tau^1)}{\partial r_1} = 2\frac{\partial p_1}{\partial z_1}.$$

Equation (1.25) implies that $p_1 = p_1(z_1, t_1)$ and thus (1.26) yields

(1.27) $$\tau^1 = r_1 \frac{\partial p_1}{\partial z_1}.$$

From the last relation we see that the scaled wall shear, $\tau_w^1 = \tau_1(1, z_1, t_1)$, is given by

(1.28) $$\tau_w^1 = \frac{\partial p_1}{\partial z_1}.$$

The constitutive equation for τ^1 when $\epsilon_2 = 0^+$:

(1.29) $$\tau^1 = \frac{\partial w_1}{\partial r_1}$$

together with the scaled form of $(\mathrm{BC})_2$:

(1.30) $$w_1(1, z_1, t_1) = -\frac{(4F-1)}{4}\tau_w^1$$

implies that

(1.31) $$w_1(r_1, z_1, t_1) = \left(-\frac{1}{4} - F + \frac{r_1^2}{2}\right)\tau_w^1, \; 0 < r_1 < 1,$$

and that

(1.32) $$\bar{w}_1(z_1, t_1) = 2\int_0^1 w_1(r_1, z_1, t_1) r_1 \, dr_1 = -F\tau_w^1.$$

If we multiply (1.24) by r_1, integrate the resulting equation from $r_1 = 0$ to $r_1 = 1$, and exploit the fact that $r_1 u_1$ vanishes at $r_1 = 0$ and $r_1 = 1$ we obtain the following equation for $p_1(z, t_1)$ and $\bar{w}(z_1, t_1)$:

$$\frac{\partial p_1}{\partial t_1} + \frac{\partial \bar{w}_1}{\partial z_1} = 0. \tag{1.33}$$

From this last identity and (1.24) we also obtain

$$\frac{1}{r_1}\frac{\partial}{\partial r_1}(r_1 u_1) = \frac{\partial}{\partial z_1}(\bar{w}_1 - w_1) \tag{1.34}$$

where w_1 and $\bar{w}_1$ are given by (1.31) and (1.32). Equation (1.34) may be integrated by quadrature yielding

$$u_1(r_1, z_1, t_1) = \frac{\partial}{\partial z_1}\left(\frac{1}{r_1}\int_0^{r_1}(\bar{w}_1(z_1, t_1) - w_1(s, z_1, t_1))s\,ds\right). \tag{1.35}$$

The above equation guarantees that as $r_1 \to 0^+$, $\frac{u_1(r_1, z_1, t_1)}{r_1}$ converges to $\frac{1}{2}\frac{\partial}{\partial z_1}(\bar{w}_1(z_1, t_1) - w(0, z_1, t))$, a finite limit. The existence of such a limit was required in order that the stresses σ^v_{rr}, $\sigma^v_{\theta\theta}$, and σ^v_{33} were finite at the center line of the capillary. We also note that $\int_0^1(\bar{w}(z_1, t_1) - w_1(s, z_1, t_1))s\,ds = 0$ and thus, as defined, u_1 does meet the boundary condition $\lim_{r_1 \to 1^-} u_1(r_1, z_1, t_1) = 0$.

To summarize, our remaining equations for p_1 and $\bar{w}_1$ are (1.28), (1.32), and (1.33). To these, we adjoin the scaled versions of (1.8) and (1.9) for the evolution of F. We write the constants D_1 and D_2 of (1.8) as

$$D_1 = p_0 c_1 \quad \text{and} \quad D_2 = p_0 c_2 \tag{1.36}$$

and observe that (1.8) and (1.9) transform to

$$\lambda \frac{dF}{dt_1} = \begin{cases} F_2 - F; & |\tau^1_w| > \mathcal{S}(\bar{w}_1) \\ \frac{1}{4} - F; & |\tau^1_w| < \mathcal{S}(\bar{w}_1) \end{cases} \tag{1.37}$$

where

$$\mathcal{S}(\bar{w}_1) = \begin{cases} c_1, & \bar{w}_1 < c_1/4 \\ c_1 + \frac{(c_2 - c_1)}{(F_2 c_2 - c_1/4)}(\bar{w}_1 - c_1/4), & \frac{c_1}{4} \le \bar{w}_1 \le F_2 c_2 \\ c_2, & F_2 c_2 < \bar{w}_1 \end{cases} \tag{1.38}$$

and

$$\lambda = \frac{T_0 R^2 p_0}{\epsilon_1 \eta_1 L^2} \tag{1.39}$$

and again T_0 is the fixed relaxation time appearing in (1.9). These equations may be

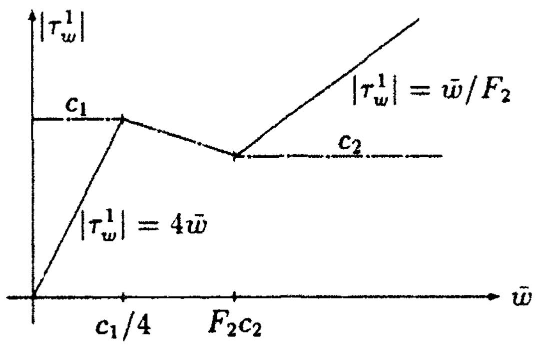

Figure 4.

combined to yield the following system for p_1 and F

$$\text{(D)} \qquad \frac{\partial p_1}{\partial t_1} - \frac{\partial}{\partial z_1}\left(F\frac{\partial p_1}{\partial z_1}\right) = 0$$

and

$$\text{(F)} \qquad \lambda\frac{\partial F}{\partial t_1} = \begin{cases} F_2 - F, & -\frac{\partial p_1}{\partial z_1} > \mathcal{S}\left(-F\frac{\partial p_1}{\partial z_1}\right) \\ \frac{1}{4} - F, & -\frac{\partial p_1}{\partial z_1} < \mathcal{S}\left(-F\frac{\partial p_1}{\partial z_1}\right) \end{cases}$$

where again $\mathcal{S}$ is given by (1.38). This latter system is solved in $0 < z_1 < 1$, the normalized region of the center line of the capillary, subject to the following boundary conditions:

$$\text{(BC)} \qquad -F(0,t_1)\frac{\partial p_1}{\partial z_1}(0,t_1) = q > 0 \quad \text{and} \quad p_1(1,t_1) = 1.$$

The condition at $z_1 = 0$ corresponds to the fact that the input of material from the reservoir to the pipe is done at a constant rate and the latter condition expresses the fact that at the pipe exit the material is at atmospheric pressure.

2. Analysis of (D), (F), and (BC)

Our interest here is in the analysis of the system

$$\text{(D)} \qquad \frac{\partial p}{\partial t} - \frac{\partial}{\partial z}\left(F\frac{\partial p}{\partial z}\right) = 0, \quad 0 < z < 1$$

$$\text{(F)} \qquad \lambda\frac{\partial F}{\partial t} = \begin{cases} F_2 - F, & -\frac{\partial p}{\partial z} > \mathcal{S}\left(-F\frac{\partial p}{\partial z}\right) \\ \frac{1}{4} - F, & -\frac{\partial p}{\partial z} < \mathcal{S}\left(-F\frac{\partial p}{\partial z}\right) \end{cases}$$

where again

$$(\mathcal{S}) \qquad \mathcal{S}(\bar{w}) = \begin{cases} c_1, & \bar{w} < c_1/4 \\ c_1 + \frac{(c_2 - c_1)}{(F_2 c_2 - c_1/4)}(\bar{w} - \frac{c_1}{4}), & c_1/4 \le \bar{w} \le F_2 c_2 \,. \\ c_2, & F_2 c_2 < \bar{u} \end{cases}$$

These equations are solved subject to the boundary and initial conditions

$$(\mathrm{BC}) \qquad -F(0,t)\frac{\partial p}{\partial z}(0,t) = q > 0 \quad \text{and} \quad p(1,t) = 1$$

and

$$(\mathrm{IC}) \qquad p(z,0^+) = p_0(z) > 0 \quad \text{and} \quad F(z,0^+) = F_0(z) \in (1/4, F_2),\ 0 < z < 1.$$

In this section we drop the subscript 1 for normalized dimensionless quantities.

It is not particularly difficult to demonstrate, either analytically or computationally, that if the parameter q in (BC) satisfies $q < c_1/4$, then solution of (D), (F), (BC), and (IC) converges to the stable equilibrium

$$(2.1) \qquad p_\infty(z) = 1 + 4q(1-z) \quad \text{and} \quad F_\infty(z) \equiv 1/4,\ 0 \le z \le 1,$$

whereas if q satisfies $q > F_2c_2$, then p converges to $1 + q(1-z)/F_2$ and F to F_2. Thus we shall confine our attention to the situation where $q \in (c_1/4, F_2c_2)$ for it is in this range that we see the oscillatory flows.

We use an operator splitting technique to integrate the system (D), (F), (BC), and (IC). If δ is our time step, we assume we have an approximate solution $(p^n, F^n)(z)$ defined at $t_n = n\delta$, $n = 0, 1, \ldots$. During the first half step we advance p keeping F fixed; that is, we solve

$$(2.2) \qquad \frac{\partial p}{\partial t} - \frac{\partial}{\partial z}\left(F\frac{\partial p}{\partial z}\right) = 0 \quad \text{and} \quad \lambda\frac{\partial F}{\partial t} = 0,\ 0 \le t \le \delta$$

subject to the boundary condition (BC) and the initial condition

$$(2.3) \qquad (p, F)(z, 0) = (p^n, F^n)(z),\ 0 < z < 1.$$

We denote the solution to (2.2), (BC), and (2.3) at $t = \delta$ by $(p^{1/2}, F^{1/2})(z)$ and of course $F^{1/2}(z) = F^n(z)$. During the second half step we solve

$$(2.4) \qquad \frac{\partial p}{\partial t} = 0 \quad \text{and} \quad \lambda\frac{\partial F}{\partial t} = \begin{cases} F_2 - F, & -\frac{\partial p}{\partial z} > \mathcal{S}\left(-F\frac{\partial p}{\partial z}\right) \\ \frac{1}{4} - F, & -\frac{\partial p}{\partial z} < \mathcal{S}\left(-F\frac{\partial p}{\partial z}\right) \end{cases}$$

subject to the initial condition

$$(2.5) \qquad (p, F)(z, 0) = (p^{1/2}, F^n)(z),\ \ 0 \le z \le 1.$$

The solution to this latter problem at $t = \delta$ is the new approximate solution at time $(n+1)\delta$.

In solving (2.2) and (2.4) we let n be an integer, $h = \frac{2}{2n+1}$, and evaluate p and F at the respective grid points $z_k^1 = \frac{2k-1}{2}h$ and $z_k^2 = (k-1)h$; $1 \le k \le (n+1)$. We use a fully implicit first order method on both (2.2) and (2.4). This allows us to choose δ and h independently and have a stable integration scheme.

We have run a number of simulations on this system with a variety of parameter values $(F_2, q_0, c_2, c_1, \lambda)$ and shall report on a few of these at the end of this section. Before doing this though, we report on one finding which surprised us. We observed that once regular oscillations had been established (and transients had died out) that the pressure field was approximately linear at each instant of time; that is the p profile was approximately given by

$$p \simeq p_{\text{lin}} \stackrel{\text{def}}{=} p_0(t) + (1 - p_0(t))z. \tag{2.6}$$

This observation suggested that a simplified model of the oscillatory flows should be possible. Below we present such a model which exploits (2.6).

If we integrate (D) from $z = 0$ to $z = 1$ and exploit the fact that the solution to (D) is approximately given by (2.6), we find that p_0 must satisfy

$$\frac{1}{2}\frac{dp_0}{dt} = (F(1,t) - F(0,t))(1 - p_0(t)). \tag{2.7}$$

Here, we are exploiting $\dfrac{\partial p}{\partial z} \simeq \dfrac{\partial p_{\text{lin}}}{\partial z} = (1 - p_0)$. A consistent interpretation of the boundary condition

$$-F(0,t)\frac{\partial p}{\partial z}(0,t) = q \tag{BC}$$

is that

$$-F(0,t)(1 - p_0(t)) = q \tag{2.8}$$

and thus (2.7) reduces to

$$\frac{1}{2}\frac{dp_0}{dt} = q - F(1,t)(p_0(t) - 1). \tag{2.9}$$

The equation for $F(1,t)$ is obtained from equation (F); we merely replace $-\dfrac{\partial p}{\partial z}(1,t)$ by $-\dfrac{\partial p_{\text{lin}}}{\partial z}(1,t) = (p_0(t) - 1)$ and obtain

$$\lambda\frac{dF}{dt}(1,t) = \begin{cases} F_2 - F(1,t), & (p_0(t) - 1) > \mathcal{S}(F(1,t)(p_0(t) - 1)) \\ \frac{1}{4} - F(1,t), & (p_0(t) - 1) < \mathcal{S}(F(1,t)(p_0(t) - 1)). \end{cases} \tag{2.10}$$

The system (2.9) and (2.10) is the simplified model used to describe the oscillatory flows. For each $q \in (\frac{c_1}{4}, c_2 F_2)$, the solutions of (2.9) and (2.10) converge to a unique orbitally stable limit cycle whose particular character depends on the choice of parameters $(\lambda, q, F_2, c_1, c_2)$. Below we show two figures. Both were run with

$$(\lambda_1, F_2, c_1, c_2) = (.5, .5, 1.95, 1.85) \tag{2.11}$$

In Figure 5

$$q = .7 \tag{2.12}$$

and in Figure 6

$$q = .6. \tag{2.13}$$

In the top portrait of each Figure the horizontal axis represents the exit flow velocity, $\bar{w}_{\text{exit}}(t)$, which is computed by

$$\bar{w}_{\text{exit}}(t) = F(1,t)(p_0(t) - 1) \tag{2.14}$$

and the vertical axis represents the pressure drop across the tube, $p_0(t) - 1$. The closed curve in each figure is the stable limit cycle for the indicated parameter values and these demonstrate the sensitivity of the oscillations to the incoming value of the flow, q. The bottom graphs of each Figure show the time histories of the pressure drop and exit velocity.

Figure 7 represents a simulation of the full system (D), (F), (BC), and (IC) run with the same parameter values used to generate Figure 6. In these simulations $n = 100$ (and thus $dx \simeq .01$) and $dt = .005$. In the top portrait of Figure 7 we have shown (1) the limit cycle for the reduced system with the parameter values used for Figure 6, (2) a graph of the pressure drop $(p(0,t)-1)$ versus the exit velocity $\bar{w}(1,t) = -F(1,t)\frac{\partial p}{\partial z}(1,t)$, and (3) a graph of minus the exit pressure gradient, $-\frac{\partial p}{\partial z}(1,t)$, versus the exit velocity $\bar{w}(1,t) = -F(1,t)\frac{\partial p}{\partial z}(1,t)$. The pressure drop curve is the narrower of these two. The second set of pictures in Figure 7 shows time histories of these quantities. In the graph labeled "pressure drop vs time" the time history of $-\frac{\partial p}{\partial z}(1,t)$ is the curve with the largest oscillations.

Figures 8–39 show snapshots of relevant flow variables at the time indicated in each figure. The data shown in Figure 8 was also used to generate Figure 7. The only pictures requiring some explanation are the ones labeled "shear vs velocity". Recalling that the normalized wall shear, $\tau_w < 0$, satisfies $|\tau_w| = -\frac{\partial p}{\partial z}(z,t)$ and that the normalized mean velocity, $\bar{w}(z,t)$, is given by $\bar{w}(z,t) = -F(z,t)\frac{\partial p}{\partial z}(z,t)$, we obtain the graphs under discussion by plotting the curves $z \to (-F(z,t)\frac{\partial p}{\partial z}(z,t), -\frac{\partial p}{\partial z}(z,t))$, $0 \le z \le 1$, at the times indicated. The points labeled x are the images of $z = 1$ and those labeled o are the images of $z = 0$ at the indicated times.

3. Conclusions

We have produced a robust model which is capable of producing relaxation oscillations which are qualitatively similar to those observed in polymer extrusion experiments. The heart of the model is the switch rule (1.8) and (1.9) which allows us to go from the slip to the no slip boundary condition at the capillary wall. Though we have not done it here, we believe it is possible to go from the linear constitutive equations employed here to more realistic ones for a molten polymer and to modify the linear slip boundary condition to one employing a nonlinear relation between the velocity at the wall and the the wall shear which is scaled by a dimensionless factor F which obeys a transition mechanism similar to (1.8) and (1.9). Our colleagues at the Ecole Nationale Superieure des Mines de Paris are currently pursuing this work.

References

[1] J.F.A. Agassant, P. Avenas, P. Sergent, and P.J. Carreau. *Polymer processing: principles and modeling.* Hanser Verlag, Munich, 1991.

[2] V. Durand, B. Vergnes, and J.F.A. Agassant. *An experimental study of HDPE melt flow instabilities.* International Congress of Rheology, Brussel, 1992.

[3] J.P. Tordella. in *Rheology*, Ririch, F.R. Ed. Academic Press, New York, 1969.

[4] C.J. Petrie and M.M. Denn. AIChE J. 22, 209, 1976.

[5] E. Boudreaux and J.A. Cuculo. J. Macromol. Sci., 16, 39, 1977–1978.

[6] J.L. Den Otter. Plast. Polym., 38, 155, 1970.

[7] P. Beaufils, B. Vergnes, and J.F. Agassant. Int. Polym. Proc., 4, 78, 1989.

[8] N. El Kissi. *These de Doctorat.* INPG, Grenoble, France, 1989.

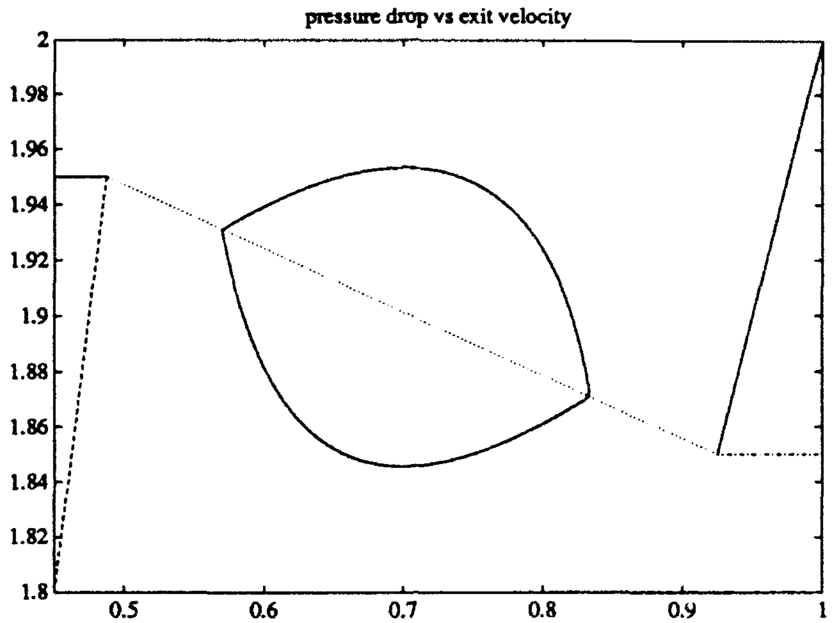

Figure 5: lambda=.5, q=.7, F2=.5, C1=1.95, C2=1.85

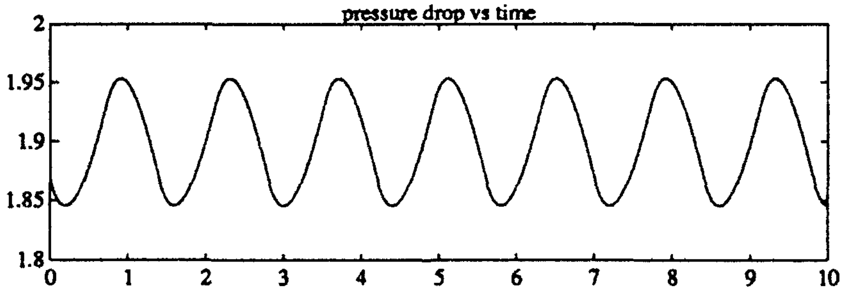

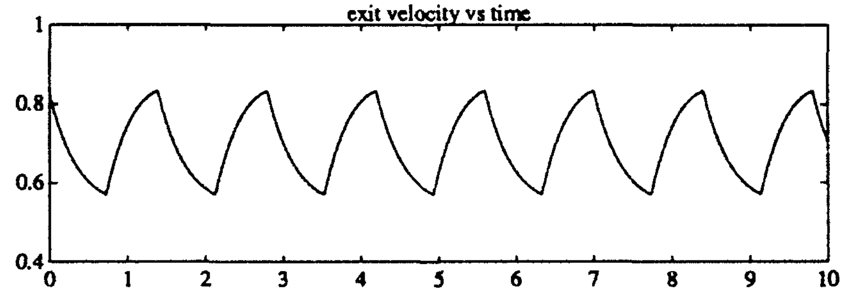

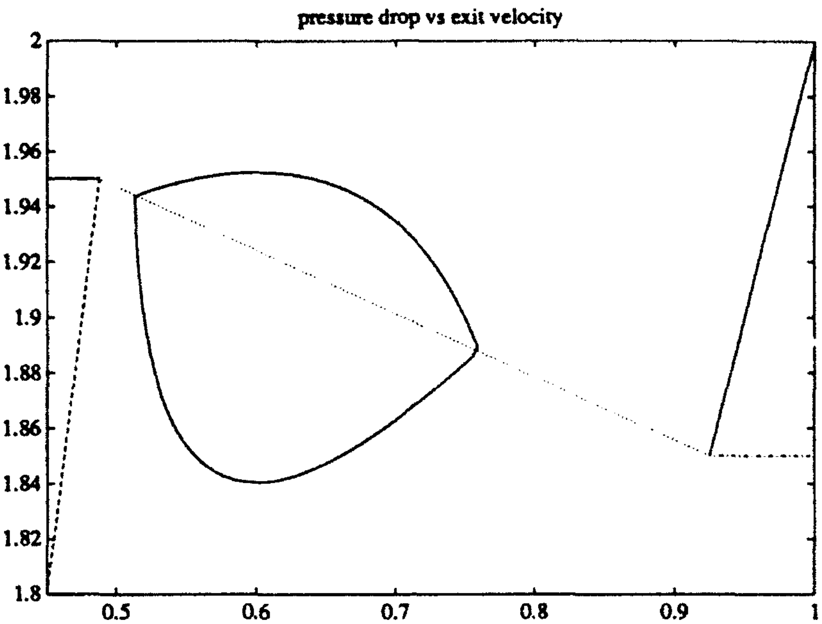

Figure 6: lambda=.5, q=.6, F2=.5, C1=1.95, C2=1.85

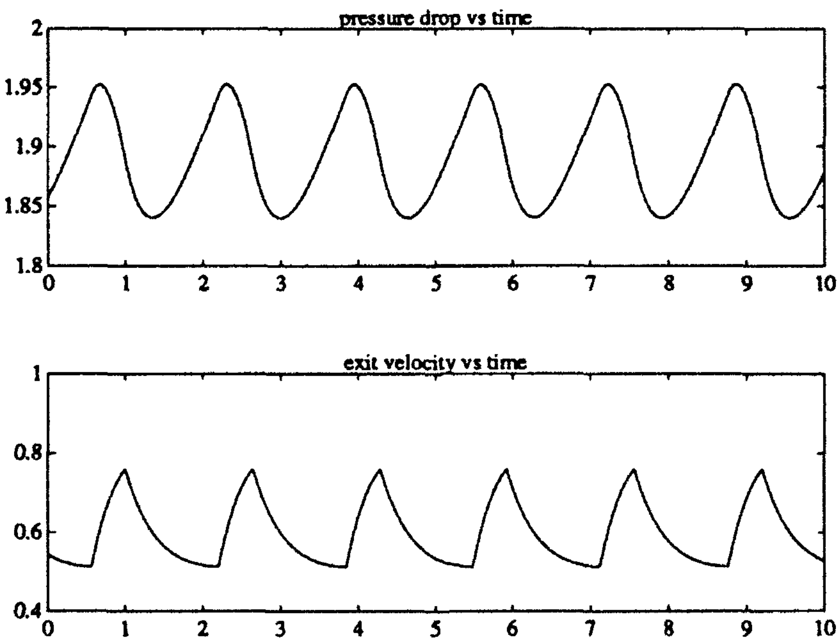

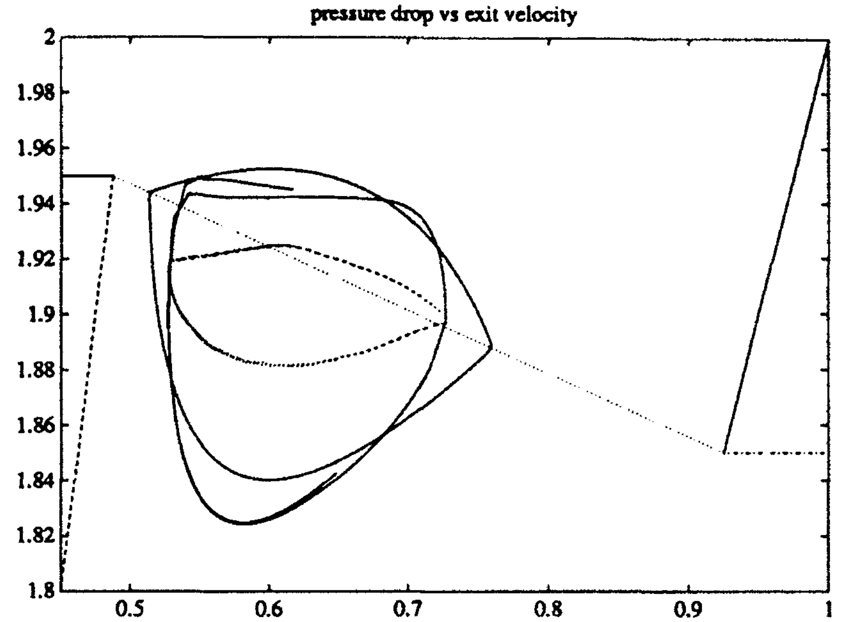

Figure 7: lambda=.5, q=.6, F2=.5, C1=1.95, C2=1.85, dx=.01, dt=.005

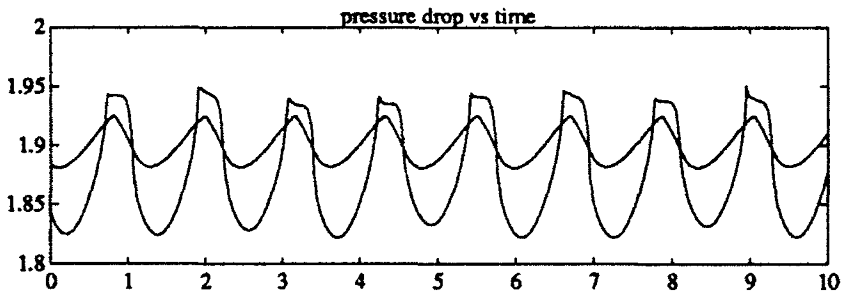

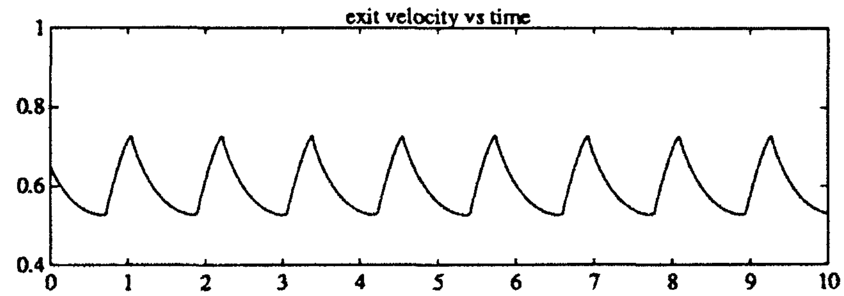

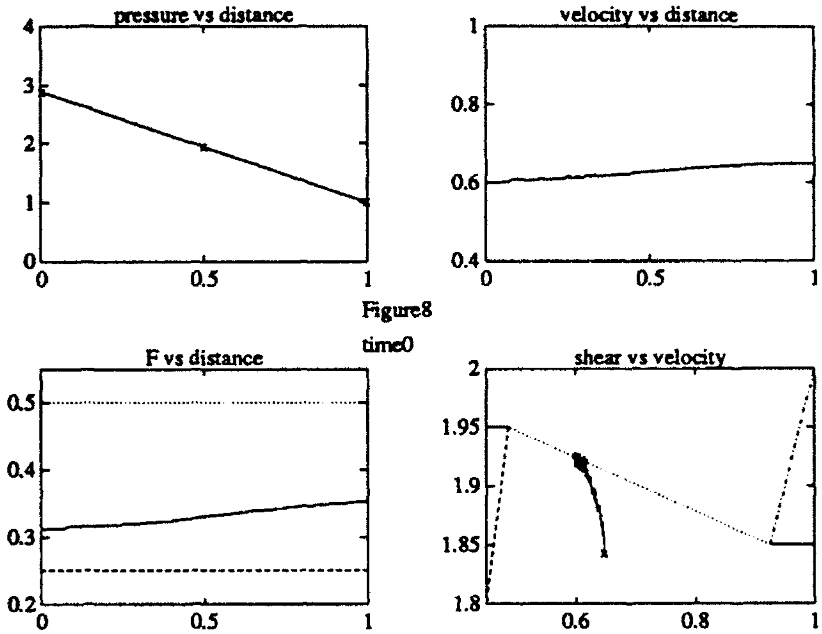

Figure8
time0

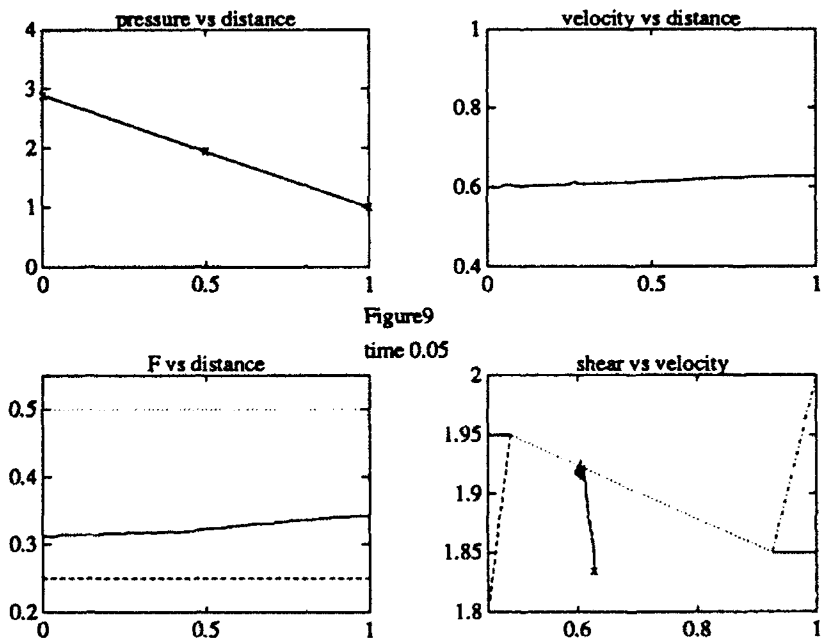

Figure9
time 0.05

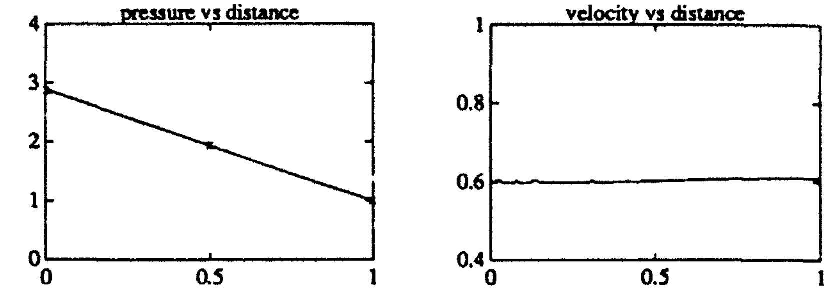

Figure10
time 0.1

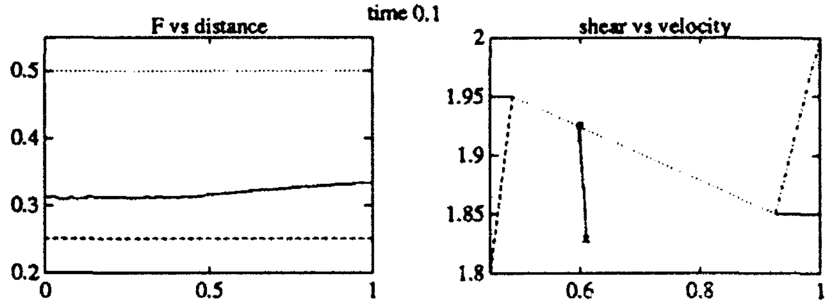

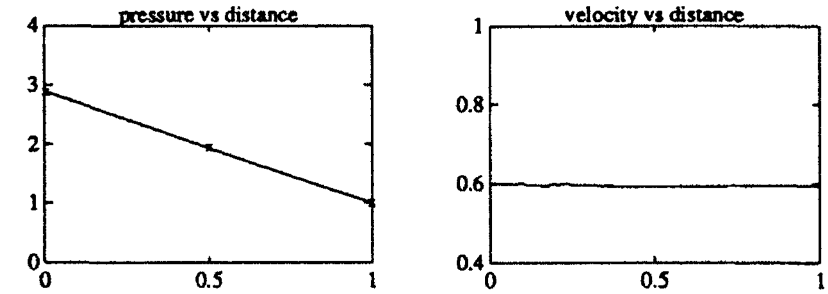

Figure11
time 0.15

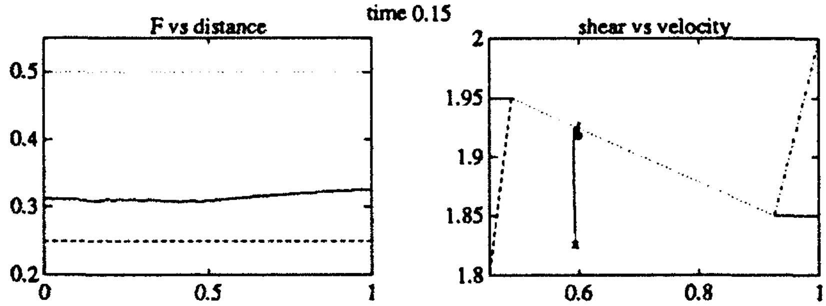

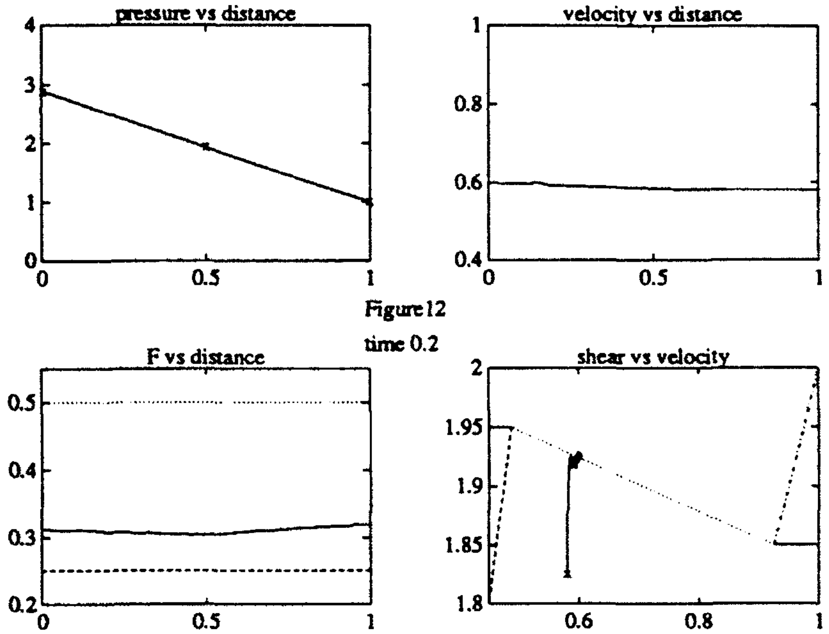

Figure12
time 0.2

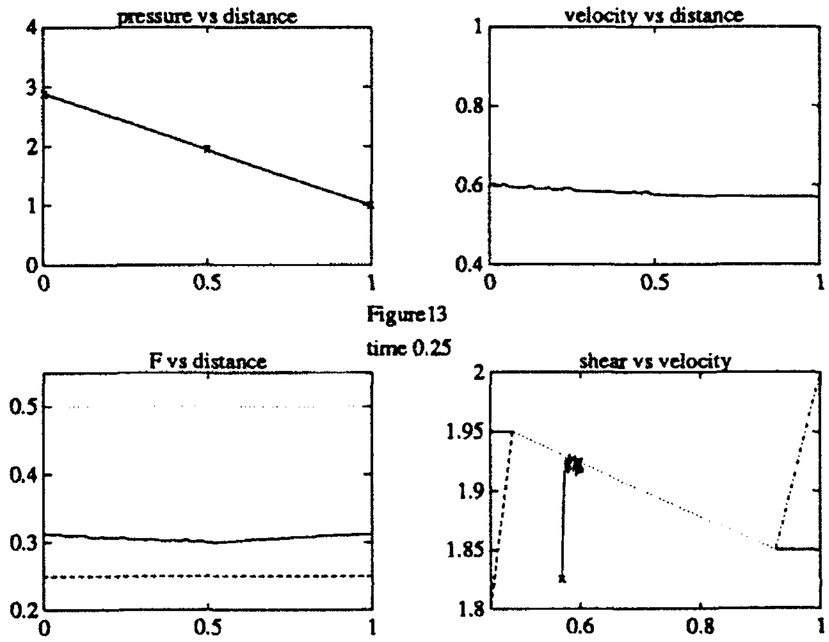

Figure13
time 0.25

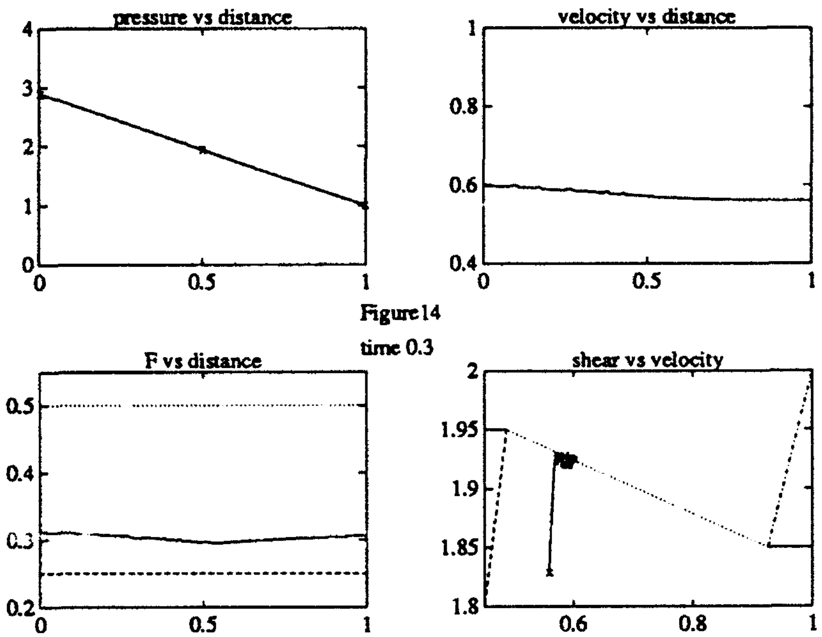

Figure 14
time 0.3

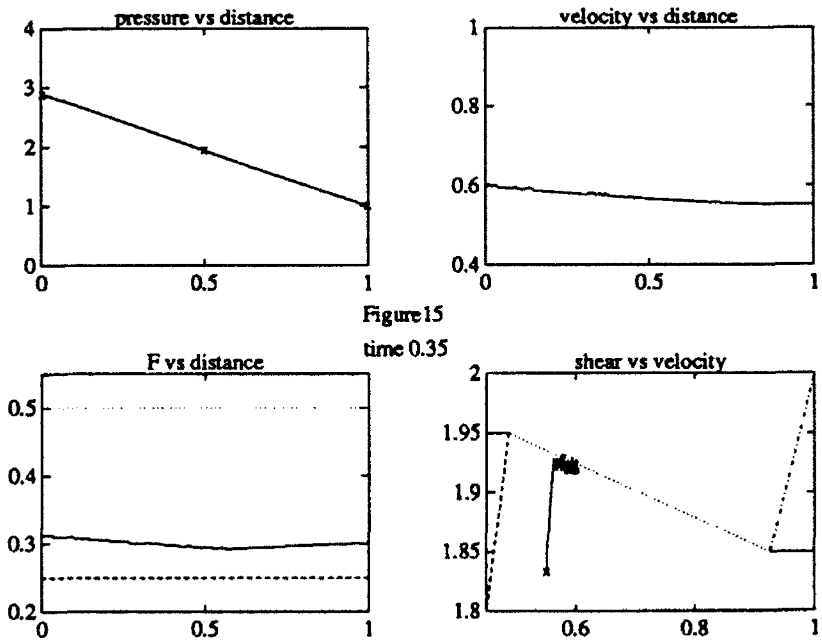

Figure 15
time 0.35

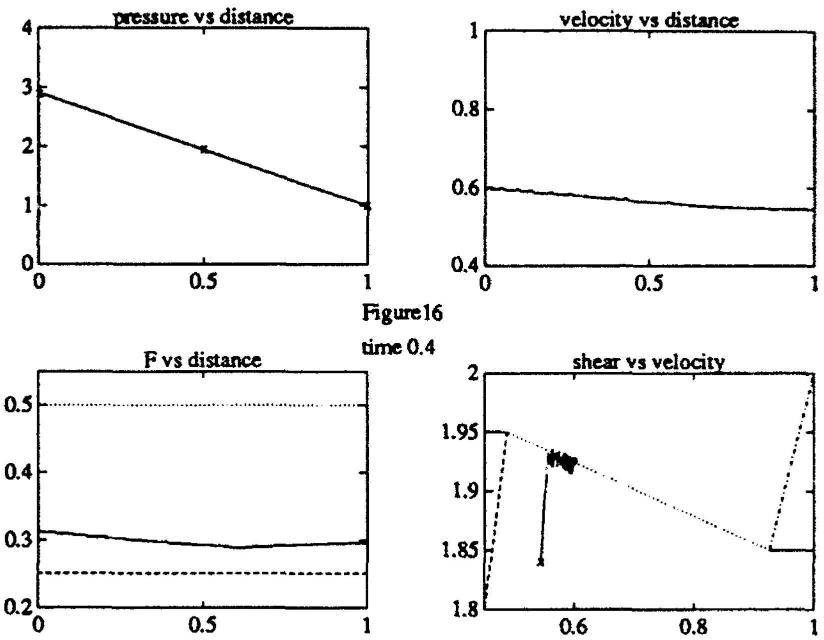

Figure16
time 0.4

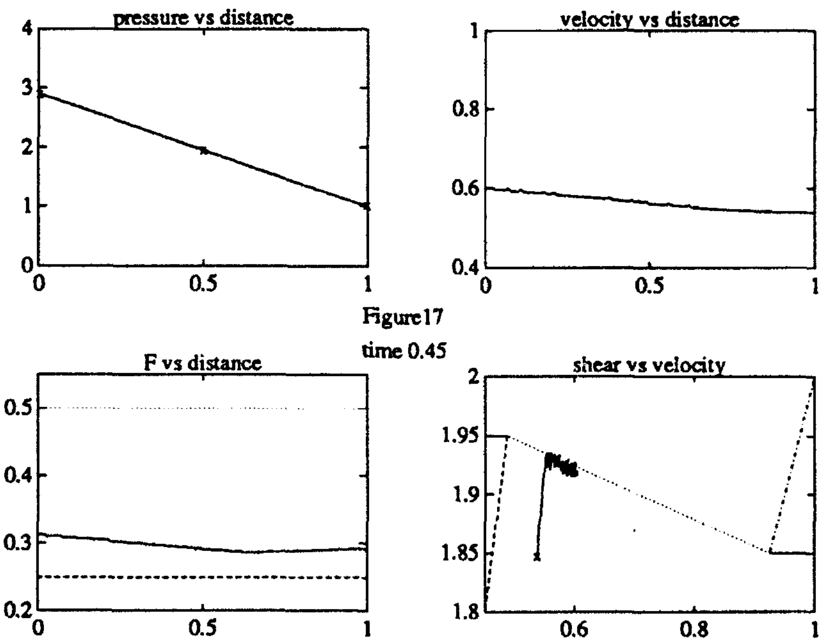

Figure17
time 0.45

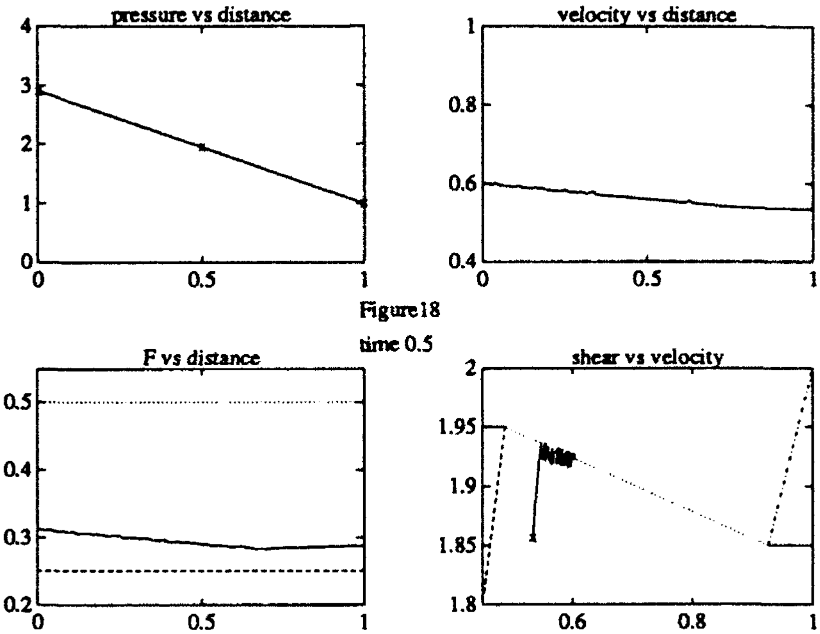

Figure18
time 0.5

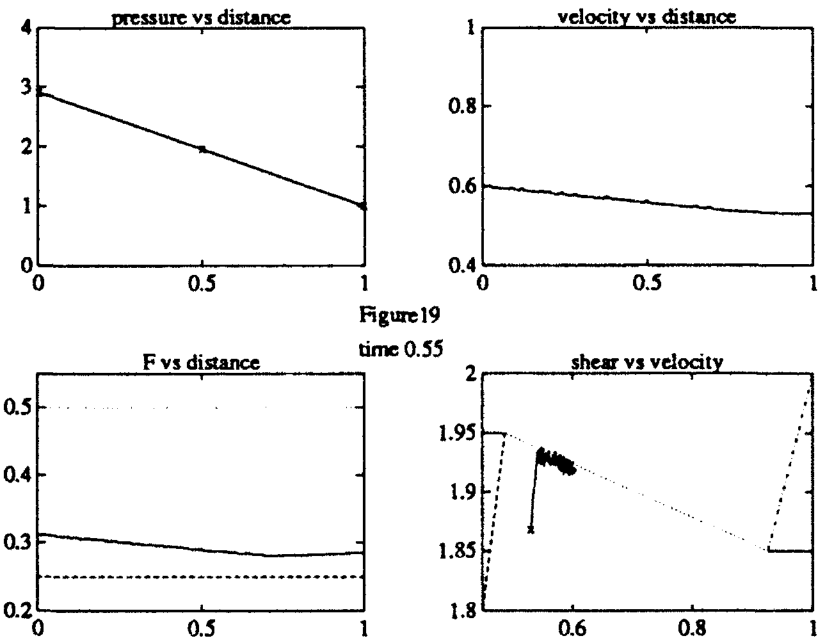

Figure19
time 0.55

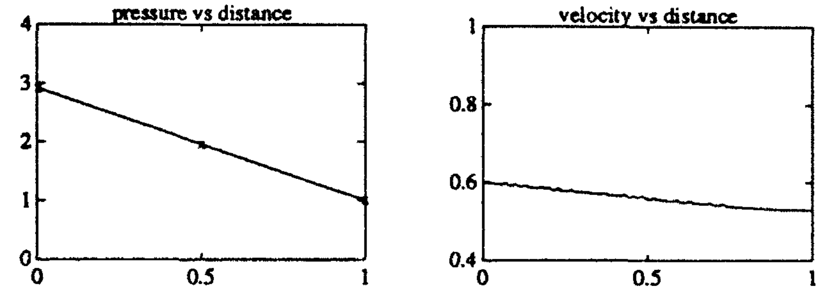

Figure20
time 0.6

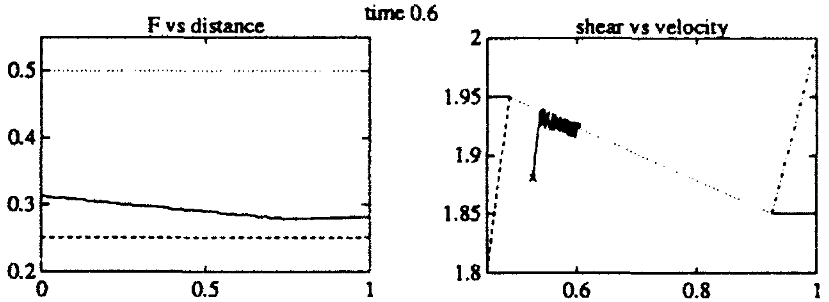

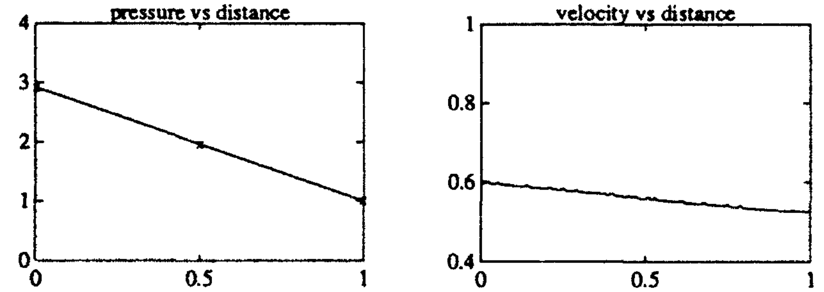

Figure21
time 0.65

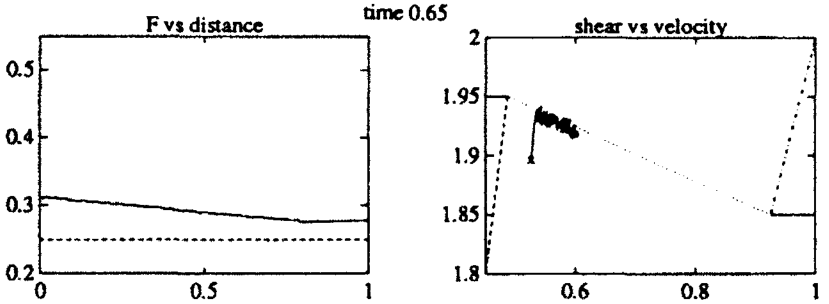

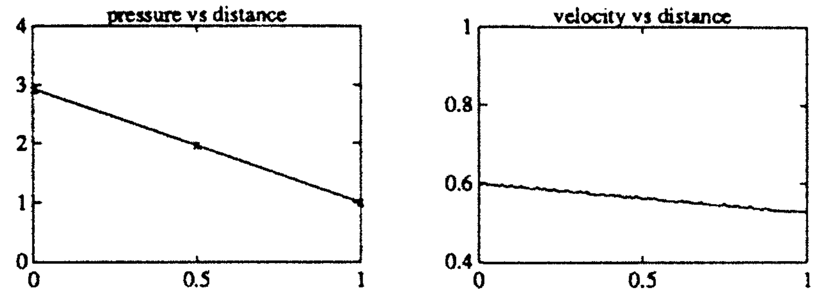

Figure22
time 0.7

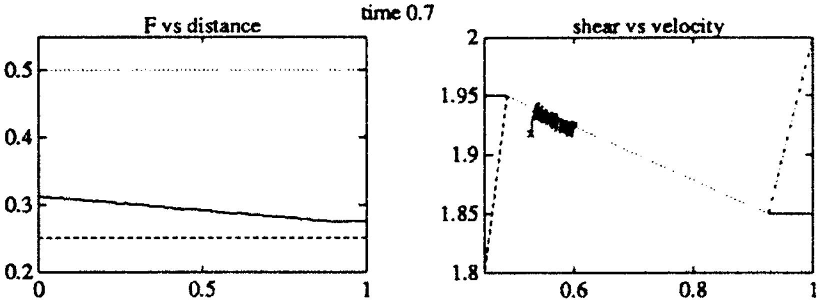

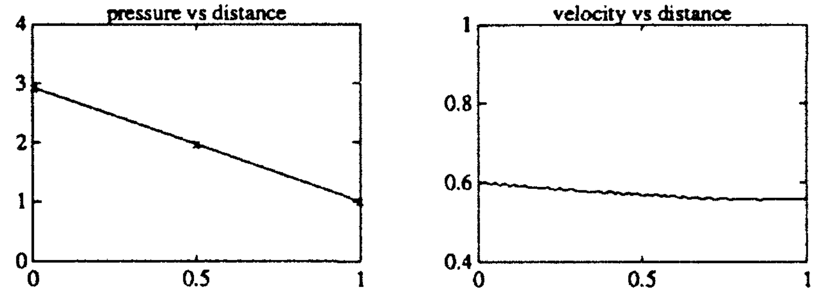

Figure23
time 0.75

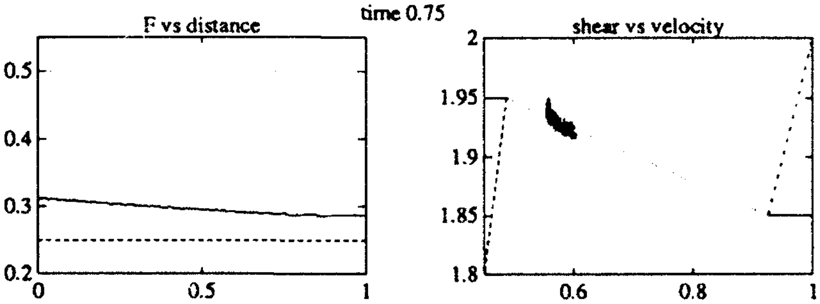

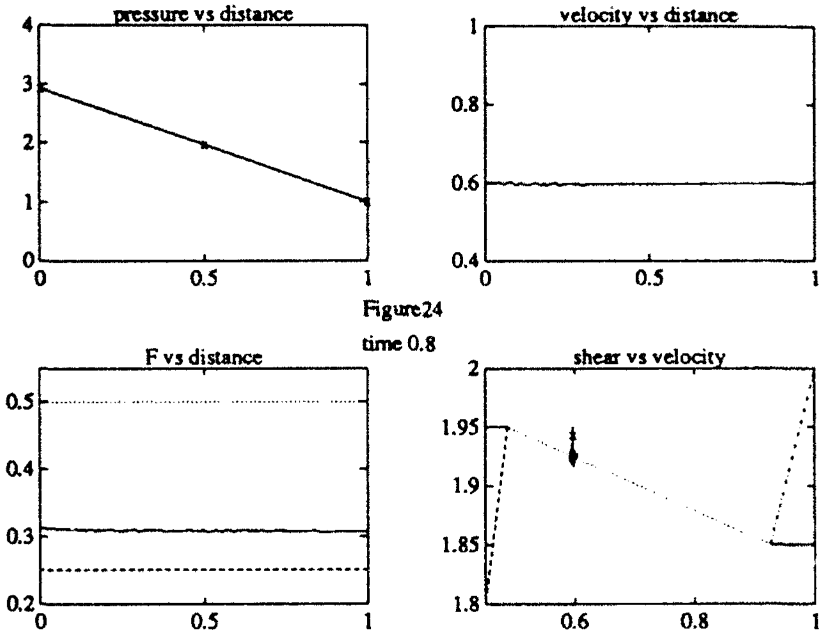

Figure24
time 0.8

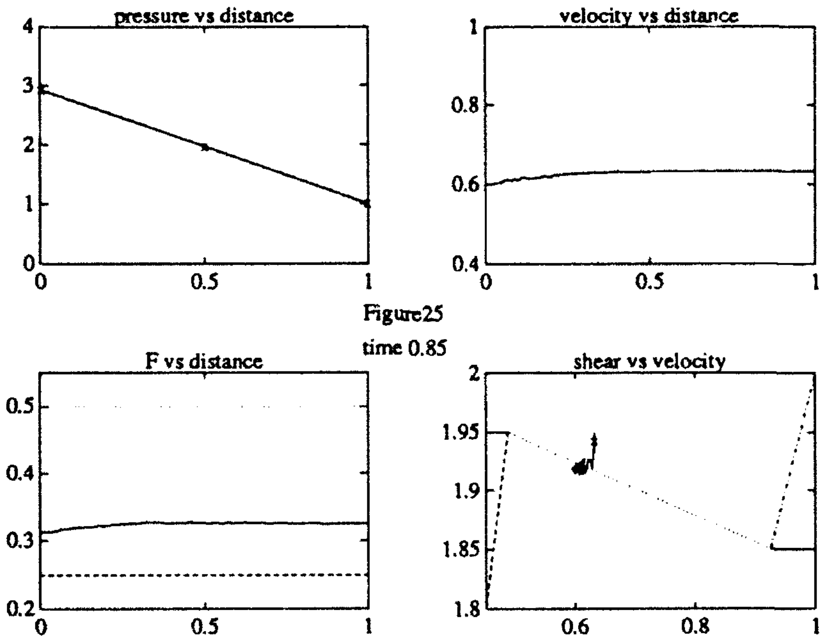

Figure25
time 0.85

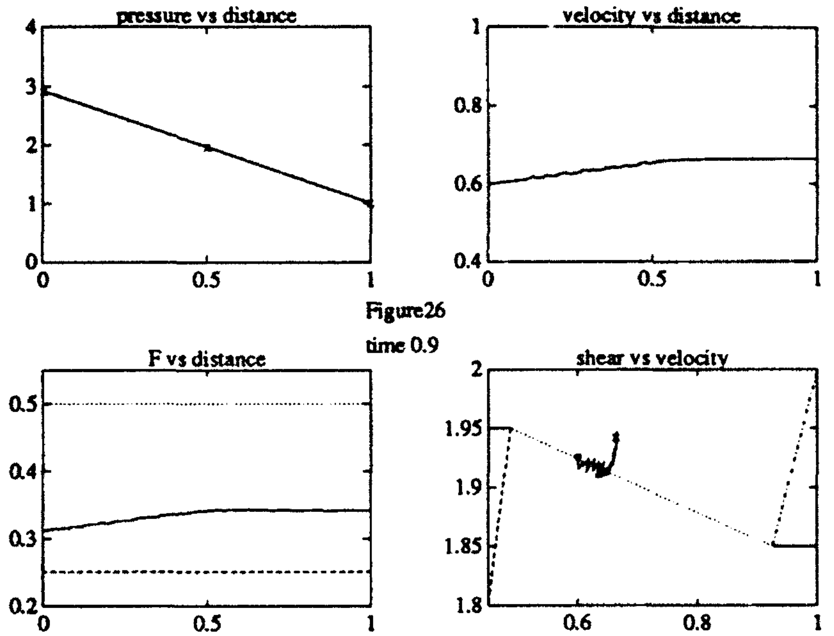

Figure26
time 0.9

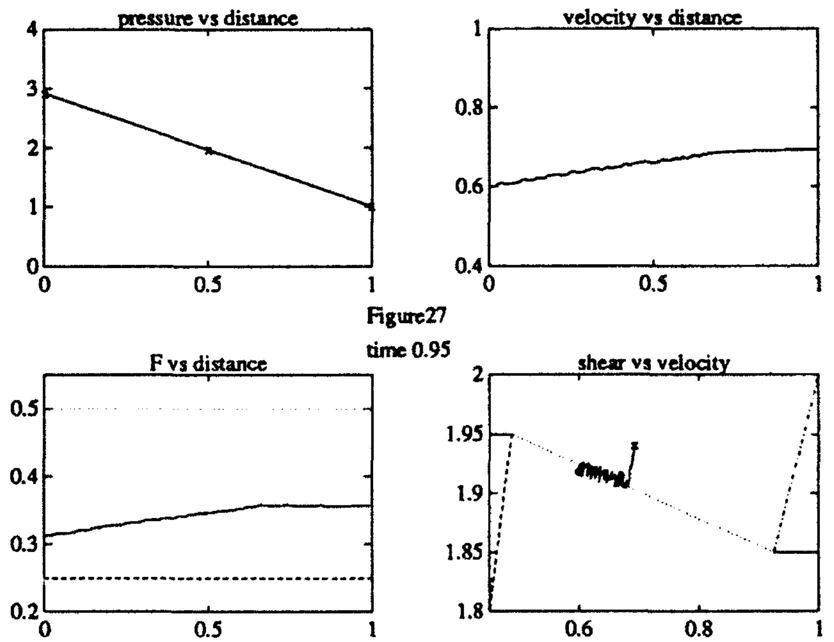

Figure27
time 0.95

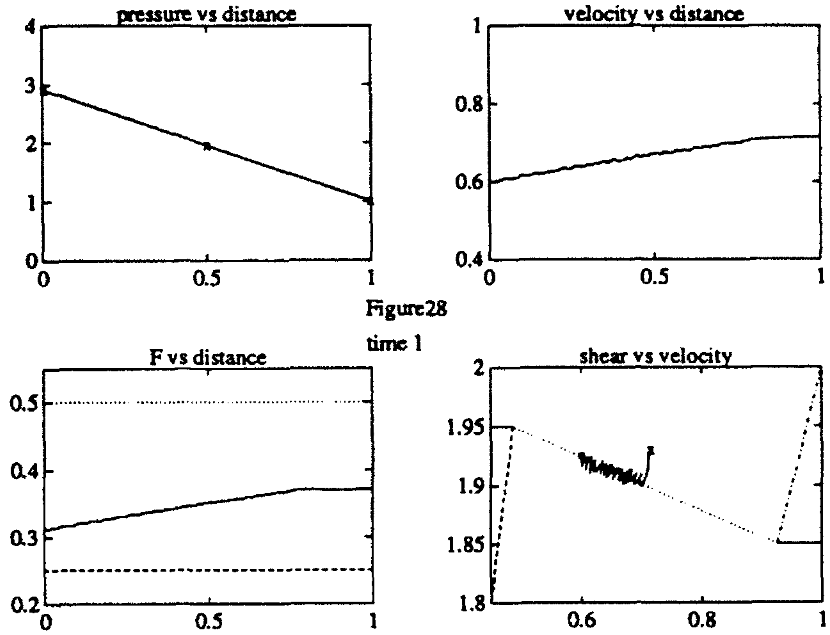

Figure28
time 1

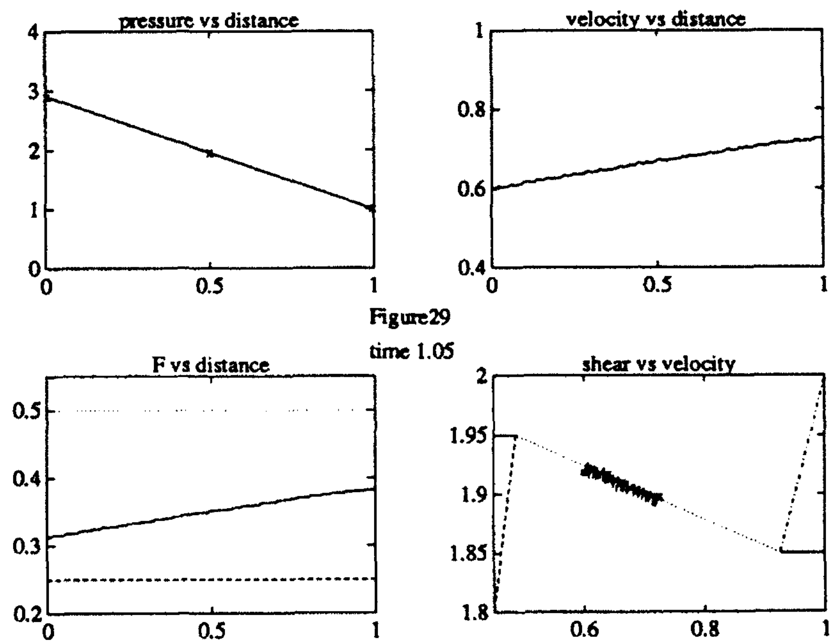

Figure29
time 1.05

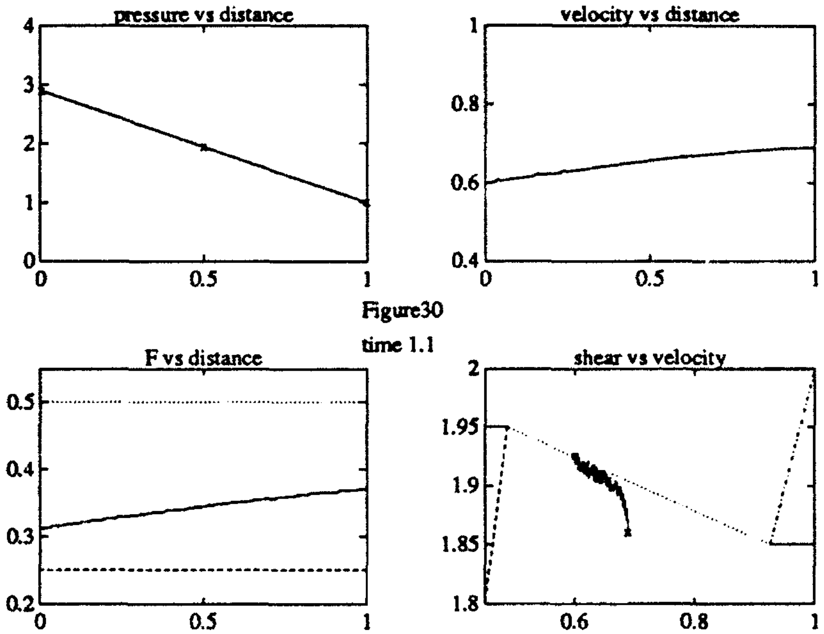

Figure30

time 1.1

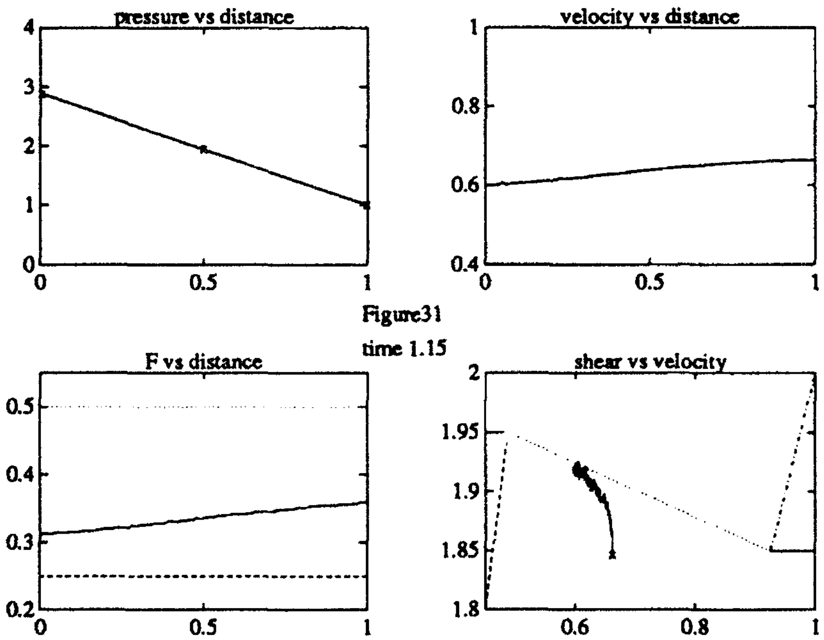

Figure31

time 1.15

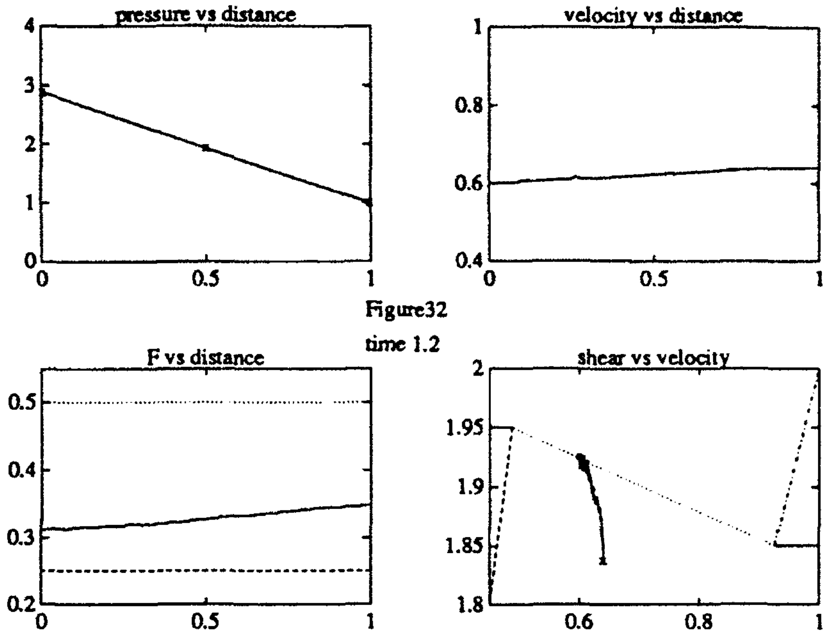

Figure32
time 1.2

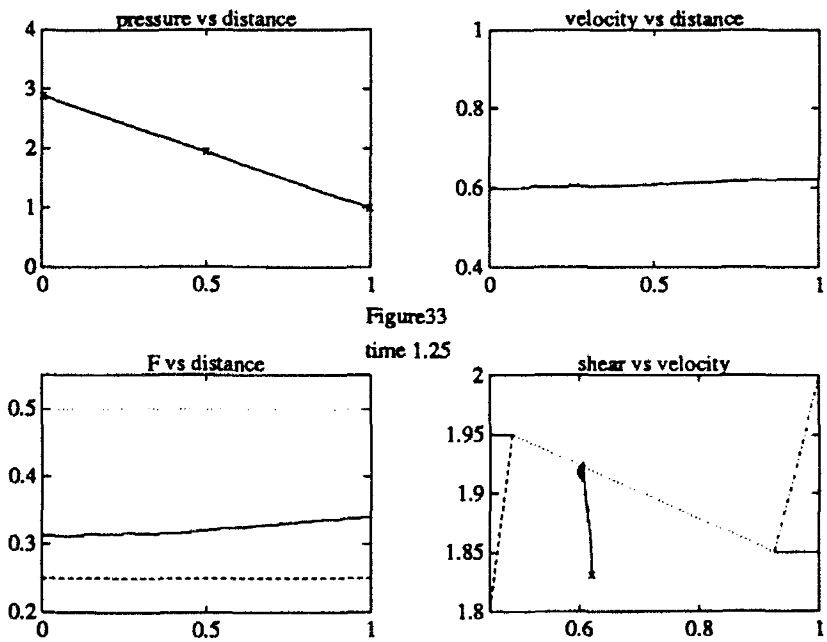

Figure33
time 1.25

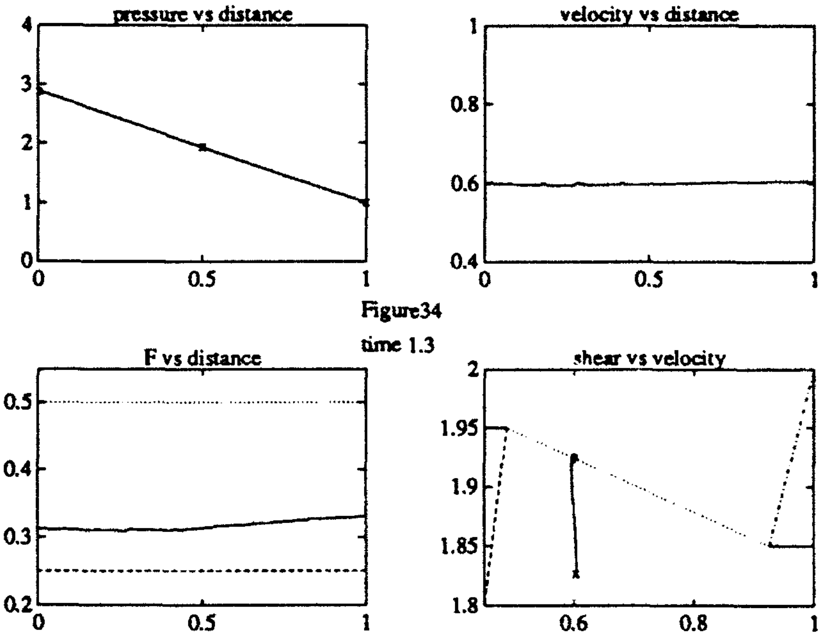

Figure34
time 1.3

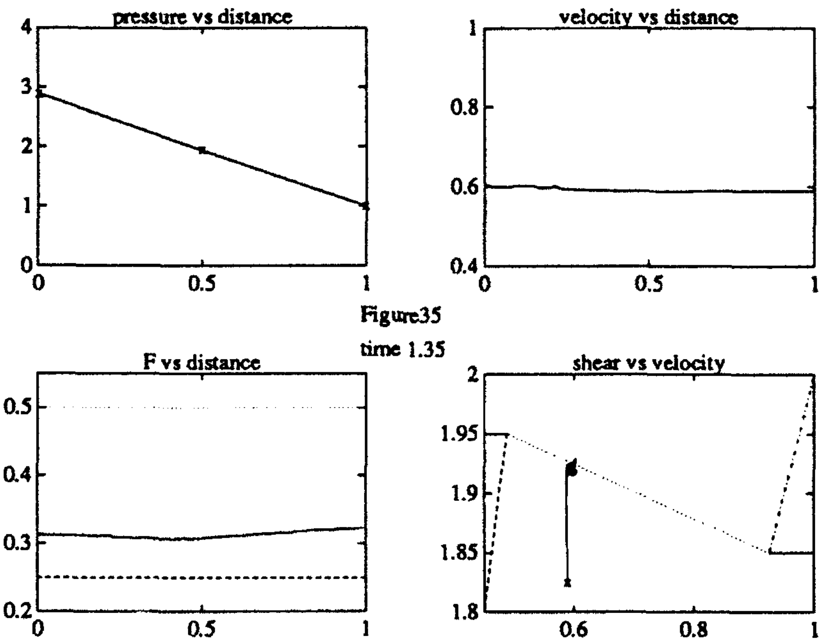

Figure35
time 1.35

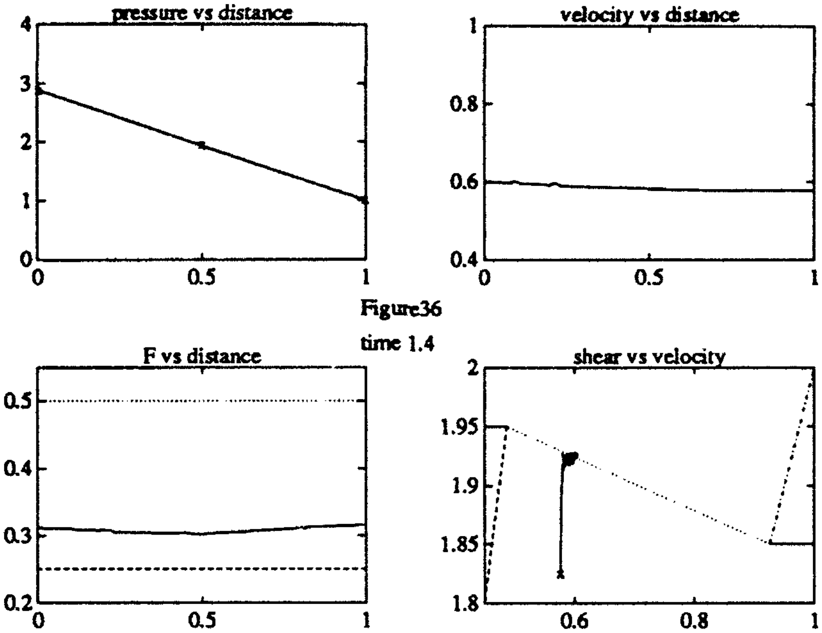

Figure36
time 1.4

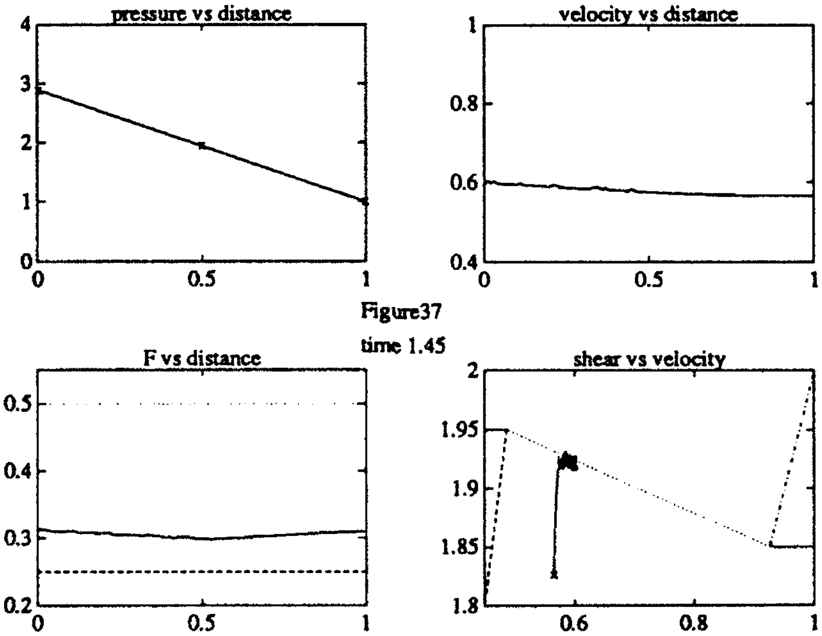

Figure37
time 1.45

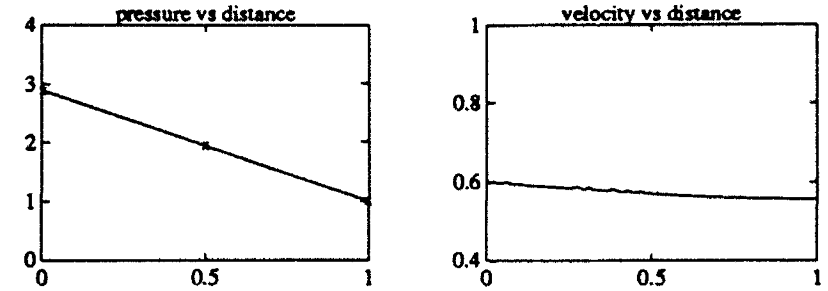

Figure38
time 1.5

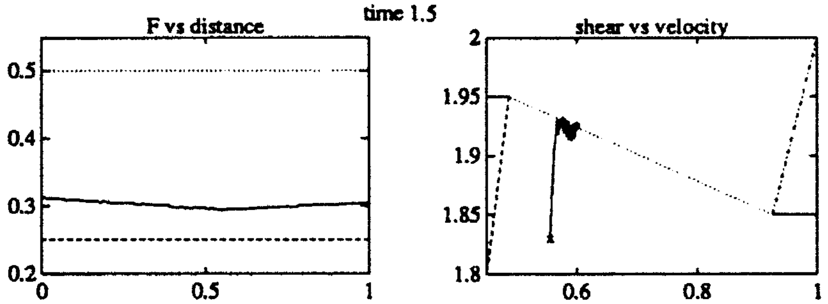

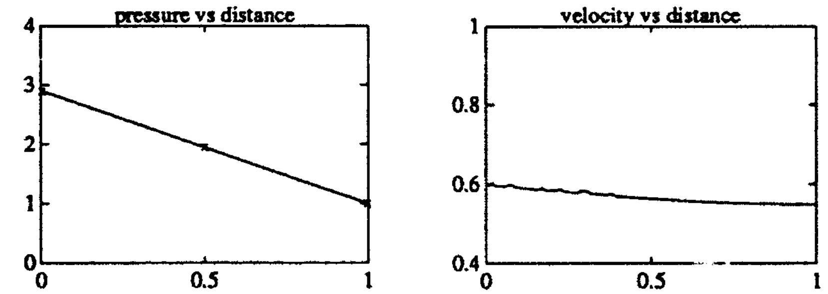

Figure39
time 1.55

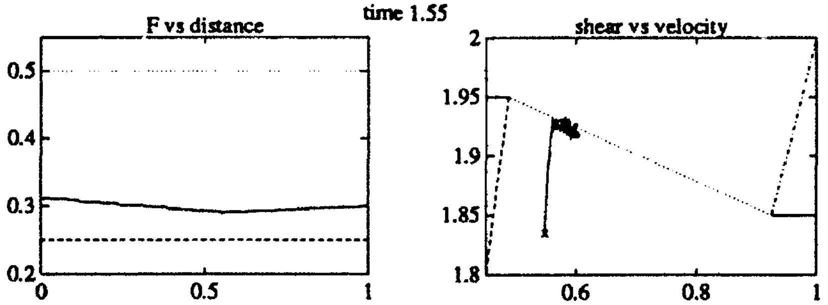

SIAM J. MATH. ANAL.
Vol. 24, No 4, pp 000–000, July 1993

ANTIPLANE SHEARING MOTIONS OF A VISCO-PLASTIC SOLID*

J. M. GREENBERG† AND ANNE NOURI‡

Abstract. The authors consider antiplane shearing motions of an incompressible isotropic visco-plastic solid. The flow rule employed is a properly invariant generalization of Coulomb sliding friction and assumes a constant yield stress or threshold above which plastic flow occurs. In this model stresses above yield are possible; but when this condition obtains, the plastic flow rule forces the plastic strain to change so as to lower the stress levels in the material and dissipate energy. On the yield surface, the flow rule looks like the classical one for a rate independent elastic-perfectly plastic material when the velocity gradients are small enough but differs from the classical model for large gradients.

Key words. plastic waves, visco-plasticity, time-dependent problems

AMS subject classifications. 73E70, 73E60, 73E50

1. Introduction. In this note we consider antiplane shearing motions of an incompressible isotropic visco-plastic solid. This work generalizes and compliments earlier work of Greenberg [1], [2], where he considered simple shearing flows for such materials. The flow rule we employ is a properly invariant generalization of Coulomb sliding friction and assumes a constant yield stress or threshold above which plastic flow occurs. As with most such theories, we assume a multiplicative decomposition of the deformation gradient into an elastic and plastic part, and we assume further that the deviatoric part of the Cauchy Stress tensor depends only on the elastic portion of the deformation gradient. For antiplane shearing motions this decomposition presents no precedence problems; i.e., does the elastic deformation precede the plastic or vice versa? One key feature of this model is that stresses above yield are possible. When this condition obtains, the plastic flow rule forces the plastic strain to change so as to lower the stress levels in the material and dissipate energy. The principal difficulty in formulating this model occurs when the stress is at yield. Motivated by results of Seidman [3], Utkin [4], and Filippov [5] on sliding modes induced by discontinuous vector fields, we are led to the flow rule advanced in (2.38). On the yield surface, this flow rule looks like the classical one for a rate independent elastic-perfectly plastic material when the velocity gradients are small enough but differs from the classical model for large gradients. This rule differentiates between loading and unloading and generates an energy identity which guarantees that uniqueness obtains for initial and initial-boundary value problems.

The organization of this paper is as follows. In §2 we develop the appropriate equations describing antiplane shearing flows in visco-plastic solids. Section 3 focuses on the uniqueness issue. Our basic estimate is that the energy associated with the difference between two solutions generated by the same data is nonincreasing. This estimate relies in an essential way on the definition of the plastic flow rule. In §4 we examine a one-dimensional signalling problem and discuss (1) the structure of this

* Received by the editors March 17, 1992; accepted for publication (in revised form) September 2, 1992.

† Department of Mathematics and Statistics, University of Maryland, Baltimore County, Baltimore, Maryland 21228. This author's research was partially supported by the U.S. National Science Foundation and the U.S. Department of Energy.

‡ Université de Nice, Parc Valrose, 06034 Nice Cedex, France. This author's research was partially supported by Centre National de la Rechereche Scientifique, France.

solution, and (2) a procedure to analytically obtain an approximate solution. We also compare this solution with what obtains for the more studied model of a rate independent elastic-perfectly plastic material where uniqueness fails. Section 5 deals with a numerical experiment for a two-dimensional signalling problem in the corner domain $r > 0$ and $\pi/2 < \theta < 2\pi$. Here the stresses are singular as one approaches the corner and care must be taken in the implementation of the boundary conditions.

We note that in the last several years there have been a number of other efforts aimed at capturing the essence of plastic flows. Antman and Szymczak [6], [7] have advanced a finite deformation theory of such materials which is similar in spirit to ours but differs in a number of essential ways. Their model is formally rate independent where ours is not but their model also requires a history dependent strain hardening mechanism. The predictions of the two theories are often qualitatively different; these differences arise since in their model the imposition of large loads tends to elevate the yield stress and create a temporally constant permanent plastic deformation, whereas in our model such loading would generate a constant plastic deformation rate and thus a plastic deformation which varies linearly in time. This may be seen by examining the solution constructed in §4. Other efforts on elasto-plastic modelling may be found in Coleman and Owen [8], Buhite and Owen [9], Coleman and Hodgdon [10], and Owen [11].

2. Model development. We say that a body is undergoing antiplane shear if material points $\xi = \xi_1\mathbf{e}_1 + \xi_2\mathbf{e}_2 + \xi_3\mathbf{e}_3$ move to $\mathbf{x} = x_1\mathbf{e}_1 + x_2\mathbf{e}_2 + x_3\mathbf{e}_3$ with

$$x_1 = \xi_1, \quad x_2 = \xi_2, \quad \text{and } x_3 = \xi_3 + \phi(\xi_1, \xi_2, t) \tag{2.1}$$

under the action of a Cauchy stress tensor of the form

$$\begin{aligned} T = &-\pi(\mathbf{e}_1 \otimes \mathbf{e}_1 + \mathbf{e}_2 \otimes \mathbf{e}_2 + \mathbf{e}_3 \otimes \mathbf{e}_3) \\ &+(S_{11}\mathbf{e}_1 \otimes \mathbf{e}_1 + S_{22}\mathbf{e}_2 \otimes \mathbf{e}_2 + S_{33}\mathbf{e}_3 \otimes \mathbf{e}_3) \\ &+S_{31}(\mathbf{e}_1 \otimes \mathbf{e}_3 + \mathbf{e}_3 \otimes \mathbf{e}_1) + S_{32}(\mathbf{e}_2 \otimes \mathbf{e}_3 + \mathbf{e}_3 \otimes \mathbf{e}_2). \end{aligned} \tag{2.2}$$[1]

Here, π is the hydrostatic pressure and S is the deviatoric stress tensor and satisfies

$$\operatorname{trace}(S) = S_{11} + S_{22} + S_{33} = 0. \tag{2.3}$$

Relative to the above basis, the matrix representation of the Cauchy stress is given by

$$\mathcal{J} = -\pi \begin{pmatrix} 1 & 0 & 0 \\ 0 & 1 & 0 \\ 0 & 0 & 1 \end{pmatrix} + \begin{pmatrix} S_{11} & 0 & S_{31} \\ 0 & S_{22} & S_{32} \\ S_{31} & S_{32} & S_{33} \end{pmatrix}, \tag{2.4}$$

and relative to the same basis the deformation gradient is given by

$$\mathcal{F} = \begin{pmatrix} 1 & 0 & 0 \\ 0 & 1 & 0 \\ F_{31} & F_{32} & 1 \end{pmatrix}, \tag{2.5}$$

---

[1] $\mathbf{e}_1 = \begin{pmatrix} 1 \\ 0 \\ 0 \end{pmatrix}$, $\mathbf{e}_2 = \begin{pmatrix} 0 \\ 1 \\ 0 \end{pmatrix}$, and $\mathbf{e}_3 = \begin{pmatrix} 0 \\ 0 \\ 1 \end{pmatrix}$ are the standard basis elements for R^3 and $\mathbf{e}_i \otimes \mathbf{e}_j = \mathbf{e}_i\mathbf{e}_j^{\mathsf{T}}$ are the standard basis elements for linear operators from R^3 to R^3.

where

$$F_{31} = \frac{\partial \phi}{\partial x_1} \quad \text{and} \quad F_{32} = \frac{\partial \phi}{\partial x_2}. \tag{2.6}$$

Noting that matrices

$$\mathcal{F}_{(a,b)} :\stackrel{\text{def}}{=} \begin{pmatrix} 1 & 0 & 0 \\ 0 & 1 & 0 \\ a & b & 1 \end{pmatrix}$$

satisfy the commutation relation

$$\mathcal{F}_{(a_1,b_1)}\mathcal{F}_{(a_2,b_2)} = \mathcal{F}_{(a_2,b_2)}\mathcal{F}_{(a_1,b_1)} = \mathcal{F}_{(a_1+a_2,b_1+b_2)}, \tag{2.7}$$

we feel justified in decomposing the deformation gradient $\mathcal{F}$ into its elastic and plastic parts $\mathcal{E}$ and $\mathcal{P}$ by

$$\mathcal{E} :\stackrel{\text{def}}{=} \begin{pmatrix} 1 & 0 & 0 \\ 0 & 1 & 0 \\ e_{31} & e_{32} & 1 \end{pmatrix} \quad \text{and} \quad \mathcal{P} :\stackrel{\text{def}}{=} \begin{pmatrix} 1 & 0 & 0 \\ 0 & 1 & 0 \\ p_{31} & p_{32} & 1 \end{pmatrix}, \tag{2.8}$$

where

$$\mathcal{F} = \mathcal{E}\mathcal{P} = \mathcal{P}\mathcal{E} = \begin{pmatrix} 1 & 0 & 0 \\ 0 & 1 & 0 \\ e_{31}+p_{31} & e_{32}+p_{32} & 1 \end{pmatrix}. \tag{2.9}$$

For such antiplane shear flows one need not make any assumption about the precedence of the elastic and plastic parts of the flow.

Our basic constitutive assumption is that under a change of reference frame E transforms in the same way as F and that the deviatoric stress S is an isotropic, frame indifferent, trace free function of the elastic deformation gradient E.[2] The constraint that S is an isotropic, frame indifferent function of E implies that S must have the functional form

$$\mathcal{S} = \alpha I + \beta\mathcal{E}\mathcal{E}^{\top} + \gamma\mathcal{E}^{-\top}\mathcal{E}^{-1} \tag{2.10}$$

or

(2.11)[3]

$$\mathcal{S} = \alpha\begin{pmatrix} 1 & 0 & 0 \\ 0 & 1 & 0 \\ 0 & 0 & 1 \end{pmatrix} + \beta\begin{pmatrix} 1 & 0 & e_{31} \\ 0 & 1 & e_{32} \\ e_{31} & e_{32} & 1+e_{31}^2+e_{32}^2 \end{pmatrix} + \gamma\begin{pmatrix} 1+e_{31}^2 & e_{31}e_{32} & -e_{31} \\ e_{31}e_{32} & 1+e_{32}^2 & -e_{32} \\ -e_{31} & -e_{32} & 1 \end{pmatrix}$$

where α, β, and γ are functions of the invariants of $\mathcal{E}\mathcal{E}^{\top}$, in this case the scalar $e_{31}^2 + e_{32}^2$. Equation (2.4) implies that $\mathcal{S}_{21} = \mathcal{S}_{12} = 0$ and this, in turn, implies that $\gamma \equiv 0$ while the condition that $\operatorname{trace}\mathcal{S} = 0$ implies that $\alpha = -\beta(1 + ((e_{31}^2 + e_{32}^2)/3))$. Combining these identities with (2.11) yields

$$\mathcal{S} = \beta\begin{pmatrix} -\frac{1}{3}(e_{31}^2+e_{32}^2) & 0 & e_{31} \\ 0 & -\frac{1}{3}(e_{31}^2+e_{32}^2) & e_{32} \\ e_{31} & e_{32} & \frac{2}{3}(e_{31}^2+e_{32}^2) \end{pmatrix}. \tag{2.12}$$

[2] E is the tensor whose matrix representation relative to the basis elements $e_i \otimes e_j$ is given by $(2.8)_1$.

[3] For details see Gurtin [12].

In the sequel we shall assume that β is a positive constant. Equation (2.12) implies that we may regard the elements S_{31} and S_{32} as basic descriptors of our system. In terms of these $\mathcal{S}$ and $\mathcal{E}$ take the form

$$\mathcal{S} = \begin{pmatrix} -\frac{1}{3\beta}(S_{31}^2 + S_{32}^2) & 0 & S_{31} \\ 0 & -\frac{1}{3\beta}(S_{31}^2 + S_{32}^2) & S_{32} \\ S_{31} & S_{32} & \frac{2}{3\beta}(S_{31}^2 + S_{32}^2) \end{pmatrix} \tag{2.13}$$

$\frac{2}{3\beta}$

and

$$\mathcal{E} = \begin{pmatrix} 1 & 0 & 0 \\ 0 & 1 & 0 \\ \frac{S_{31}}{\beta} & \frac{S_{32}}{\beta} & 1 \end{pmatrix}. \tag{2.14}$$

We now turn to the equations of motion. Equation (2.1) implies that the Eulerian velocity field $\mathbf{u}$ is of the form

$$\mathbf{u} = u(x_1, x_2, t_1)\mathbf{e}_3, \tag{2.15}$$

where

$$u(x_1, x_2, t_1) = \frac{\partial \phi}{\partial t_1}(x_1, x_2, t_1); \tag{2.16}$$

and (2.16), when combined with (2.6), implies that

$$\frac{\partial F_{31}}{\partial t_1} - \frac{\partial u}{\partial x_1} = 0 \tag{2.17}$$

and

$$\frac{\partial F_{32}}{\partial t_1} - \frac{\partial u}{\partial x_2} = 0. \tag{2.18}$$

Additionally, (2.9) and (2.14) imply that

$$F_{31} = \frac{S_{31}}{\beta} + p_{31} \tag{2.19}$$

and

$$F_{32} = \frac{S_{32}}{\beta} + p_{32}. \tag{2.20}$$

Balance of momentum in the $\mathbf{e}_1$ and $\mathbf{e}_2$ directions implies that

$$\frac{\partial}{\partial x_1}\left(\pi + \frac{(S_{31}^2 + S_{32}^2)}{3\beta}\right) = \frac{\partial}{\partial x_2}\left(\pi + \frac{(S_{31}^2 + S_{32}^2)}{3\beta}\right) = 0 \tag{2.21}$$

or equivalently that

$$\pi = \pi_0(x_3, t) - \frac{(S_{31}^2 + S_{32}^2)}{3\beta}(x_1, x_2, t), \tag{2.22}$$

whereas balance of momentum in the $\mathbf{e}_3$ direction yields

$$\rho_0 \frac{\partial u}{\partial t_1} - \frac{\partial S_{31}}{\partial x_1} - \frac{\partial S_{32}}{\partial x_2} = -\frac{\partial \pi_0}{\partial x_3}. \tag{2.23}$$

Here, ρ_0 is the constant mass density of the material. Since $\partial\pi_0/\partial x_3$ depends on x_3 and t_1, whereas all quantities on the left-hand side of (2.23) depend only on x_1, x_2, and t_1, we conclude that for antiplane shearing flows $\partial\pi_0/\partial x_3$ is independent of x_3. In what follows we shall assume this quantity is zero.

We now turn our attention to "yield condition" and the flow rule for the plastic strain tensor $\mathcal{P}$ of $(2.8)_2$. We assume that yield is determined by whether the scalar $S_{31}^2 + S_{32}^2$ exceeds a threshold S_y^2 or not. This assumption relies on the special form of $\mathcal{S}$ (see (2.13)) and is equivalent to a yield criteria determined by the norm of $\mathcal{S}$, where

$$\|\mathcal{S}\|^2 :\stackrel{\text{def}}{=} \mathcal{S}_{ij}\mathcal{S}_{ij} = 2(S_{31}^2 + S_{32}^2) + \frac{2}{3\beta^2}(S_{31}^2 + S_{32}^2)^2 \tag{2.24}$$

or one based on the maximum shear stress

$$S_*^2 :\stackrel{\text{def}}{=} \max_{\{\mathbf{e}|\mathbf{e}\cdot\mathbf{e}=1\}} \|\mathcal{S}\mathbf{e} - (\mathcal{S}\mathbf{e}\cdot\mathbf{e})\mathbf{e}\|^2. \tag{2.25}$$

In the sequel we let H denote the Heaviside function

$$H(x) :\stackrel{\text{def}}{=} \begin{cases} 0, & x < 0 \\ 1, & x > 0 \end{cases} \tag{2.26}$$

and define ψ_1 and ψ_2 by

$$\psi_1 = \frac{1}{2}\int_{-\infty}^{(S_{31}^2+S_{32}^2)} H(x - S_y^2)\,dx \tag{2.27}$$

and

$$\psi_2 = \int_{-\infty}^{\sqrt{S_{31}^2+S_{32}^2}} H(x - S_y)\,dx. \tag{2.28}$$

where $S_y > 0$ is the "yield stress."

We shall confine our attention to the Coulomb type sliding law

$$\frac{\partial p_{31}}{\partial t_1} = \frac{1}{\beta T_0}\frac{\partial \psi_1}{\partial S_{31}} = \frac{S_{31}}{\beta T_0} H(S_{31}^2 + S_{32}^2 - S_y^2) \tag{2.29}$$

and

$$\frac{\partial p_{32}}{\partial t_1} = \frac{1}{\beta T_0}\frac{\partial \psi_1}{\partial S_{32}} = \frac{S_{32}}{\beta T_0} H(S_{31}^2 + S_{32}^2 - S_y^2), \tag{2.30}$$

though much of what we say applies equally well to the flow rule

$$\frac{\partial p_{31}}{\partial t_1} = \frac{S_y}{\beta T_0}\frac{\partial \psi_2}{\partial S_{31}} = \frac{S_y S_{31}}{\beta T_0\sqrt{S_{31}^2 + S_{32}^2}} H\left(\sqrt{S_{31}^2 + S_{32}^2} - S_y\right) \tag{2.31}$$

and

$$\frac{\partial p_{32}}{\partial t_1} = \frac{S_y}{\beta T_0}\frac{\partial \psi_2}{\partial S_{32}} = \frac{S_y S_{32}}{\beta T_0\sqrt{S_{31}^2+S_{32}^2}} H\left(\sqrt{S_{31}^2+S_{32}^2} - S_y\right). \tag{2.32}$$

The constant β is the shear modulus in (2.12), S_y is the yield stress, and $T_0 > 0$ is a fixed relaxation time. The flow rule is defined for $S_{31}^2 + S_{32}^2 \neq S_y^2$ and the problem remains to define it on the yield surface.

We first note that if $S_{31}^2 + S_{32}^2 \neq S_y^2$, we can combine (2.17)–(2.20) and (2.29) and (2.30) to obtain the following system for S_{31}, S_{32}, and u:

$$\frac{1}{\beta}\frac{\partial S_{31}}{\partial t_1} - \frac{\partial u}{\partial x_1} = \frac{-S_{31}H(S_{31}^2+S_{32}^2-S_y^2)}{\beta T_0}, \tag{2.33}$$

$$\frac{1}{\beta}\frac{\partial S_{32}}{\partial t_1} - \frac{\partial u}{\partial x_2} = \frac{-S_{32}H(S_{31}^2+S_{32}^2-S_y^2)}{\beta T_0}, \tag{2.34}$$

and

$$\rho_0\frac{\partial u}{\partial t_1} - \frac{\partial S_{31}}{\partial x_1} - \frac{\partial S_{32}}{\partial x_2} = 0. \tag{2.35}$$

Equations (2.33) and (2.34) imply that for $S_{31}^2 + S_{32}^2 \neq S_y^2$,

$$\begin{aligned}\frac{\partial}{\partial t_1}(S_{31}^2+S_{32}^2) &= 2\beta\left(S_{31}\frac{\partial u}{\partial x_1} + S_{32}\frac{\partial u}{\partial x_2}\right)\\ &\quad -\frac{2}{T_0}(S_{31}^2+S_{32}^2)H(S_{31}^2+S_{32}^2-S_y^2),\end{aligned} \tag{2.36}$$

and (2.36), together with the results of [3], [4], [5], motivates our extension of the flow rule on the yield surface $S_{31}^2 + S_{32}^2 = S_y^2$. We extend (2.29) and (2.30) to the yield surface $S_{31}^2 + S_{32}^2 = S_y^2$ by

$$\frac{\partial p_{31}}{\partial t_1} = \frac{\alpha S_{31}}{\beta T_0} \quad\text{and}\quad \frac{\partial p_{32}}{\partial t_1} = \frac{\alpha S_{32}}{\beta T_0}, \tag{2.37}$$

where

(2.38)

$$\alpha = \begin{cases} 1 \quad \text{if } S_{31}^2+S_{32}^2 = S_y^2 \quad \text{and} \quad S_{31}\dfrac{\partial u}{\partial x_1} + S_{32}\dfrac{\partial u}{\partial x_2} > \dfrac{S_y^2}{\beta T_0}, \\[2ex] \beta T_0\left(S_{31}\dfrac{\partial u}{\partial x_1} + S_{32}\dfrac{\partial u}{\partial x_2}\right)/S_y^2 \quad \text{if } S_{31}^2+S_{32}^2 = S_y^2 \quad \text{and} \\[2ex] 0 \le S_{31}\dfrac{\partial u}{\partial x_1} + S_{32}\dfrac{\partial u}{\partial x_2} \le \dfrac{S_y^2}{\beta T_0}, \\[2ex] 0 \quad \text{if } S_{31}^2+S_{32}^2 = S_y^2 \quad \text{and} \quad S_{31}\dfrac{\partial u}{\partial x_1} + S_{32}\dfrac{\partial u}{\partial x_2} < 0. \end{cases}$$ [4]

[4] The relations (2.37) and (2.38) transform in a frame indifferent fashion.

In the sequel we shall confine our attention to the extended flow rule (2.29), (2.30), (2.37) and (2.38). The relevant equations are

$$\frac{1}{\beta}\frac{\partial S_{31}}{\partial t_1} - \frac{\partial u}{\partial x_1} = -\frac{\alpha S_{31}}{\beta T_0}, \tag{2.39}$$

$$\frac{1}{\beta}\frac{\partial S_{32}}{\partial t_1} - \frac{\partial u}{\partial x_2} = -\frac{\alpha S_{32}}{\beta T_0}, \tag{2.40}$$

$$\rho_0\frac{\partial u}{\partial t_1} - \frac{\partial S_{31}}{\partial x_1} - \frac{\partial S_{32}}{\partial x_2} = 0, \tag{2.41}$$

where now

$$\alpha = \begin{cases} 1 & \text{if } S_{31}^2 + S_{32}^2 > S_y^2 \\ 1 & \text{if } S_{31}^2 + S_{32}^2 = S_y^2 \quad \text{and} \quad \dfrac{\beta T_0}{S_y^2}\left(S_{31}\dfrac{\partial u}{\partial x_1} + S_{32}\dfrac{\partial u}{\partial x_2}\right) > 1 \\ \dfrac{\beta T_0}{S_y^2}\left(S_{31}\dfrac{\partial u}{\partial x_1} + S_{32}\dfrac{\partial u}{\partial x_2}\right) & \text{if } S_{31}^2 + S_{32}^2 = S_y^2 \quad \text{and} \\ & 0 \leq \dfrac{\beta T_0}{S_y^2}\left(S_{31}\dfrac{\partial u}{\partial x_1} + S_{32}\dfrac{\partial u}{\partial x_2}\right) \leq 1 \\ 0 & \text{if } S_{31}^2 + S_{32}^2 = S_y^2 \quad \text{and} \quad \dfrac{\beta T_0}{S_y^2}\left(S_{31}\dfrac{\partial u}{\partial x_1} + S_{32}\dfrac{\partial u}{\partial x_2}\right) < 0 \\ 0 & \text{if } S_{31}^2 + S_{32}^2 < S_y^2, \end{cases} \tag{2.42}$$

and these are solved together with appropriate initial and boundary conditions. Having solved the above system for S_{31}, S_{32}, and u we recover the deformation gradients F_{31} and F_{32} by solving

$$\frac{\partial F_{31}}{\partial t_1} - \frac{\partial u}{\partial x_1} = 0 \quad \text{and} \quad \frac{\partial F_{32}}{\partial t_1} - \frac{\partial u}{\partial x_2} = 0 \tag{2.43}$$

together with appropriate initial conditions. The plastic strains p_{31} and p_{32} are then given by

$$p_{31} = F_{31} - \frac{S_{31}}{\beta} \quad \text{and} \quad p_{31} = F_{32} - \frac{S_{32}}{\beta}. \tag{2.44}$$

These equations should be contrasted with what obtains in the more commonly studied theory of rate independent elastic-perfectly plastic materials. In that theory (2.37), (2.39)–(2.41), (2.43) and (2.44) still hold but α is given by

(2.45)

$$\alpha = \begin{cases} \dfrac{\beta T_0}{S_y^2}\left(S_{31}\dfrac{\partial u}{\partial x_1} + S_{32}\dfrac{\partial u}{\partial x_2}\right) & \text{if } S_{31}^2 + S_{32}^2 = S_y^2 \quad \text{and} \\ 0 \le \dfrac{\beta T_0}{S_y^2}\left(S_{31}\dfrac{\partial u}{\partial x_1} + S_{32}\dfrac{\partial u}{\partial x_2}\right), & \\ 0 \quad \text{if } S_{31}^2 + S_{32}^2 = S_y^2 \quad \text{and} \quad \dfrac{\beta T_0}{S_y^2}\left(S_{31}\dfrac{\partial u}{\partial x_1} + S_{32}\dfrac{\partial u}{\partial x_2}\right) < 0, & \\ 0 \quad \text{if } S_{31}^2 + S_{32}^2 < S_y^2. & \end{cases}$$

The unboundedness of α on the yield surface $S_{31}^2 + S_{32}^2 = S_y^2$ presents difficulties not encountered in our model. In particular, across nonstationary shocks where F_{31}, F_{32}, u, S_{31}, and S_{32} experience jump discontinuities, we must admit jumps in the plastic strains p_{31} and p_{32}. The reason for this is that in the classical rate independent theory—α as in (2.45)—we must allow "dirac" type singularities in the terms $\alpha S_{31}/\beta T_0$ and $\alpha S_{32}/\beta T_0$ and therefore, we cannot conclude that

$$cn_1[p_{31}] = cn_2[p_{32}] = 0. \tag{2.46}$$

Here, c is the normal velocity of the shock wave and $\mathbf{n}=(n_1, n_2)$ is the unit normal to the shock. In our model α is bounded, no "dirac" type singularities arise in the terms $\alpha S_{31}/\beta T_0$ and $\alpha S_{32}/\beta T_0$, and thus (2.46) holds. This implies that with our model all nonstationary shocks satisfy $c^2 = 1$; that is, they propagate with the speed of elastic signals. With our model, the only surfaces across which the plastic strains can jump are stationary, i.e. $c = 0$. Such jumps are also allowed in the classical theory.

We conclude this section by writing down a dimensionless version (2.39)–(2.44). We let

$$\begin{gathered} x = \sqrt{\frac{\rho_0}{\beta}}\frac{x_1}{T_0}, y = \sqrt{\frac{\rho_0}{\beta}}\frac{x_2}{T_0}, t = \frac{t_1}{T_0} \\ v = \sqrt{\frac{\rho_0}{\beta}}u, \tau_{31} = \frac{S_{31}}{\beta}, \tau_{32} = \frac{S_{32}}{\beta}, \text{ and } \tau_y = \frac{S_y}{\beta} \end{gathered} \tag{2.47}$$

and observe that (2.39)–(2.42) transform to

$$\frac{\partial \tau_{31}}{\partial t} - \frac{\partial v}{\partial x} = -\hat{\alpha}\tau_{31}, \tag{2.48}$$

$$\frac{\partial \tau_{32}}{\partial t} - \frac{\partial v}{\partial y} = -\hat{\alpha}\tau_{32}, \tag{2.49}$$

$$\frac{\partial v}{\partial t} - \frac{\partial \tau_{31}}{\partial x} - \frac{\partial \tau_{32}}{\partial y} = 0, \tag{2.50}$$

where

(2.51)

$$\hat{\alpha} = \begin{cases} 1 \quad \text{if } \tau_{31}^2 + \tau_{32}^2 > \tau_y^2 \\ 1 \quad \text{if } \tau_{31}^2 + \tau_{32}^2 = \tau_y^2 \quad \text{and} \quad \dfrac{1}{\tau_y^2}\left(\tau_{31}\dfrac{\partial v}{\partial x_1} + \tau_{32}\dfrac{\partial v}{\partial x_2}\right) > 1, \\ \dfrac{1}{\tau_y^2}\left(\tau_{31}\dfrac{\partial v}{\partial x_1} + \tau_{32}\dfrac{\partial v}{\partial x_2}\right) \quad \text{if } \tau_{31}^2 + \tau_{32}^2 = \tau_y^2 \text{ and} \\ 0 \le \dfrac{1}{\tau_y^2}\left(\tau_{31}\dfrac{\partial v}{\partial x_1} + \tau_{32}\dfrac{\partial v}{\partial x_2}\right) \le 1, \\ 0 \quad \text{if } \tau_{31}^2 + \tau_{32}^2 = \tau_y^2 \quad \text{and} \quad \dfrac{1}{\tau_y^2}\left(\tau_{31}\dfrac{\partial v}{\partial x_1} + \tau_{32}\dfrac{\partial v}{\partial x_2}\right) < 0, \\ 0 \quad \text{if } \tau_{31}^2 + \tau_{32}^2 < \tau_y^2. \end{cases}$$

The transformed versions of (2.43) and (2.44) are

$$\frac{\partial F_{31}}{\partial t} - \frac{\partial v}{\partial x} = 0 \quad \text{and} \quad \frac{\partial F_{32}}{\partial t} - \frac{\partial v}{\partial y} = 0 \tag{2.52}$$

and

$$p_{31} = F_{31} - \tau_{31} \quad \text{and} \quad p_{32} = F_{32} - \tau_{32}. \tag{2.53}$$

3. Uniqueness results. Our task in this section is to establish the following

THEOREM 3.1. *Let Ω be an open domain in $\mathbb{R}^2$ with smooth boundary $\partial\Omega$. Then, there is at most one piecewise smooth,*[5] *$L^2_{\text{loc}}(\Omega)$ solution $(\tau_{31}, \tau_{32}, v)$ to (2.48)–(2.51) satisfying*

$$\lim_{t \to 0^+} (\tau_{31}, \tau_{32}, v)(x, y, t) = (\tau_{31}^0, \tau_{32}^0, v^0)(x, y), \tag{3.1}$$

$$\lim_{(x,y)\in\Omega; (x,y)\to\partial\Omega_1} (n_1\tau_{31} + n_2\tau_{32})(x, y, t) = f_1(x, y, t), \tag{3.2}$$

$$\lim_{(x,y)\in\Omega; (x,y)\to\partial\Omega_2} v(x, y, t) = f_2(x, y, t). \tag{3.3}$$

Here $\partial\Omega = \partial\Omega_1 \cup \partial\Omega_2$, $\partial\Omega_1 \cap \partial\Omega_2$ is at worst a finite collection of points, $\mathbf{n}=(n_1, n_2)$ is the unit exterior normal to $\partial\Omega_1$, and the functions f_i are smooth functions in $L^2_{\text{loc}}(\partial\Omega_i \times [0, \infty))$.

Proof. We first note that if $(\tau_{31}^b, \tau_{32}^b, v^b)$ and $(\tau_{31}^a, \tau_{32}^a, v^a)$ are two solutions to (2.48)–(2.51), then their differences satisfy

$$\frac{\partial}{\partial t}(\tau_{31}^b - \tau_{31}^a) - \frac{\partial}{\partial x}(v^b - v^a) = -(\hat{\alpha}^b \tau_{31}^b - \hat{\alpha}^a \tau_{31}^a), \tag{3.4}$$

$$\frac{\partial}{\partial t}(\tau_{32}^b - \tau_{32}^a) - \frac{\partial}{\partial y}(v^b - v^a) = -(\hat{\alpha}^b \tau_{32}^b - \hat{\alpha}^a \tau_{32}^a), \tag{3.5}$$

and

$$\frac{\partial}{\partial t}(v^b - v^a) - \frac{\partial}{\partial x}(\tau_{31}^b - \tau_{31}^a) - \frac{\partial}{\partial y}(\tau_{32}^b - \tau_{32}^a) = 0. \tag{3.6}$$

[5] This formulation admits shocks which propagate with normal velocity c satisfying $c^2 = 1$.

Here, $\hat{\alpha}^b$ and $\hat{\alpha}^a$ represent the bounded function $\hat{\alpha}$ defined in (2.51) evaluated at $(\tau_{31}^b, \tau_{32}^b, v^b)$ and $(\tau_{31}^a, \tau_{32}^a, v^a)$, respectively. The last three identities imply that

$$
\begin{aligned}
&\frac{1}{2}\frac{\partial}{\partial t}\left[(\tau_{31}^b-\tau_{31}^a)^2+(\tau_{32}^b-\tau_{32}^a)^2+(v^b-v^a)^2\right] \\
&\qquad -\frac{\partial}{\partial x}\left[(\tau_{31}^b-\tau_{31}^a)(v^b-v^a)\right]-\frac{\partial}{\partial y}\left[(\tau_{32}^b-\tau_{32}^a)(v^b-v^a)\right] \\
&\qquad = -\left[(\tau_{31}^b-\tau_{31}^a)(\hat{\alpha}^b\tau_{31}^b-\hat{\alpha}^a\tau_{31}^a)+(\tau_{32}^b-\tau_{32}^a)(\hat{\alpha}^b\tau_{32}^b-\hat{\alpha}^a\tau_{32}^a)\right].
\end{aligned}
\tag{3.7}
$$

We now claim that

$$
p \overset{\text{def}}{:=} (\tau_{31}^b-\tau_{31}^a)(\hat{\alpha}^b\tau_{31}^b-\hat{\alpha}^a\tau_{31}^a)+(\tau_{32}^b-\tau_{32}^a)(\hat{\alpha}^b\tau_{32}^b-\hat{\alpha}^a\tau_{32}^a)
\tag{3.8}
$$

is nonnegative. In verifying this assertion there is no loss in generality in assuming that

$$
0 \le \hat{\alpha}^a \le \hat{\alpha}^b \le 1.
\tag{3.9}
$$

We first note that p may be rewritten as

$$
\begin{aligned}
p = {} & \hat{\alpha}^a\left[(\tau_{31}^b-\tau_{31}^a)^2+(\tau_{32}^b-\tau_{32}^a)^2\right] \\
&+(\hat{\alpha}^b-\hat{\alpha}^a)\left[(\tau_{31}^b)^2-\tau_{31}^a\tau_{31}^b+(\tau_{32}^b)^2-\tau_{32}^a\tau_{32}^b\right].
\end{aligned}
\tag{3.10}
$$

If $\hat{\alpha}^a = 0$, then $(\tau_{31}^a)^2+(\tau_{32}^a)^2 \le \tau_y^2$ and $\tau_{31}^a\tau_{31}^b+\tau_{32}^a\tau_{32}^b \le \tau_y\sqrt{(\tau_{31}^b)^2+(\tau_{32}^b)^2}$ and, therefore, (3.10) implies that

$$
p \ge \hat{\alpha}^b\sqrt{(\tau_{31}^b)^2+(\tau_{32}^b)^2}\left(\sqrt{(\tau_{31}^b)^2+(\tau_{32}^b)^2}-\tau_y\right).
\tag{3.11}
$$

If $\hat{\alpha}^b = 0$, then (3.10) implies that $p = 0$, whereas if $0 < \hat{\alpha}^b \le 1$, (2.51) implies that $\sqrt{(\tau_{31}^b)^2+(\tau_{32}^b)^2} \ge \tau_y$, and (3.11) then yields $p \ge 0$. We now turn to the case where $0 < \hat{\alpha}^a \le \hat{\alpha}^b \le 1$. If $\hat{\alpha}^b = \hat{\alpha}^a$, the nonnegativity of p follows from (3.10), and thus to complete the verification that $p \ge 0$ it suffices to consider the case where $0 < \hat{\alpha}^a < \hat{\alpha}^b \le 1$. Here we know that $(\tau_{31}^a)^2+(\tau_{32}^a)^2 = \tau_y^2$ and $(\tau_{31}^b)^2+(\tau_{32}^b)^2 \ge \tau_y^2$. The former identity, along with (3.10) and $\tau_{31}^a\tau_{31}^b+\tau_{32}^a\tau_{32}^b \le \tau_y\sqrt{(\tau_{31}^b)^2+(\tau_{32}^b)^2}$, implies that

$$
\begin{aligned}
p \ge {} & \hat{\alpha}^a\left[(\tau_{31}^b-\tau_{31}^a)^2+(\tau_{32}^b-\tau_{32}^a)^2\right] \\
&+(\hat{\alpha}^b-\hat{\alpha}^a)\sqrt{(\tau_{31}^b)^2+(\tau_{32}^b)^2}\left(\sqrt{(\tau_{31}^b)^2+(\tau_{32}^b)^2}-\tau_y\right),
\end{aligned}
\tag{3.12}
$$

and (3.12), $0 < \hat{\alpha}^a < \hat{\alpha}^b \le 1$, and $(\tau_{31}^b)^2+(\tau_{32}^b)^2 \ge \tau_y^2$ complete the proof of the assertion that p is nonnegative.

For any $(x_0, y_0) \in \mathbb{R}^2$, $r_0 > 0$, $T > 0$, and $0 \le t \le T$ we let

$$
C(x_0, y_0, r_0, t) \overset{\text{def}}{:=} \{(x,y) \mid (x-x_0)^2+(y-y_0)^2 < (r_0+T-t)^2\}.
\tag{3.13}
$$

The identity (3.7) implies that if $(\tau_{31}^b, \tau_{32}^b, v^b)$ and $(\tau_{31}^a, \tau_{32}^a, v^a)$ are two solutions of (2.48)-(2.51) taking on the same data (3.1)-(3.3), then

$$
\frac{1}{2}\int_{C(x_0,y_0,r_0,T)\cap\Omega}\left((\tau_{31}^b-\tau_{31}^a)^2+(\tau_{32}^b-\tau_{32}^a)^2+(v^b-v^a)^2\right)dx\,dy
\tag{3.14}
$$

delete T replace with t

$$
\begin{aligned}
&+\int_0^T \left(\int_{C(x_0,y_0,r_0,T)\cap\Omega} p(x,y,t)\,dx\,dy \right) dt \\
&+\int_0^T \left(\int_{\partial C(x_0,y_0,r_0,T)\cap\Omega} \left(\frac{1}{2}((\tau_{31}^b-\tau_{31}^a)^2+(\tau_{32}^b-\tau_{32}^a)^2+(v^b-v^a)^2) - \right.\right. \\
&\left.\left. -(v^b-v^a)\left(\frac{(x-x_0)(\tau_{31}^b-\tau_{31}^a)}{(r_0+T-t)} + \frac{(y-y_0)(\tau_{32}^b-\tau_{32}^a)}{(r_0+T-t)} \right) \right) ds \right) dt \\
&= 0.
\end{aligned}
$$

Here,

(3.15) $$\partial C(x_0,y_0,r_0,t) = \{(x,y) \mid (x-x_0)^2+(y-y_0)^2=(r_0+T-t)^2\}.$$

The vector $((x-x_0)/(r_0+T-t),(y-y_0)/(r_0+T-t))$ is the unit exterior normal to $\partial C(x_0,y_0,r_0,t)$, and ds is arc length along $\partial C(x_0,y_0,r_0,t)$. Since

(3.16)
$$
\begin{aligned}
&-(v^b-v^a)\left(\frac{(x-x_0)(\tau_{31}^b-\tau_{31}^a)}{(r_0+T-t)} + \frac{(y-y_0)(\tau_{32}^b-\tau_{32}^a)}{(r_0+T-t)} \right) \\
&\geq -|v^b-v^a|\sqrt{(\tau_{31}^b-\tau_{31}^a)^2+(\tau_{32}^b-\tau_{32}^a)^2} \\
&\geq -\frac{1}{2}((\tau_{31}^b-\tau_{31}^a)^2+(\tau_{32}^b-\tau_{32}^a)^2+(v^b-v^a)^2)
\end{aligned}
$$

and since $p \geq 0$, we see that all three integrals in (3.15) are nonnegative and their sum is zero. From this we obtain

(3.17) $$\int_{C(x_0,y_0,r_0,T)\cap\Omega} ((\tau_{31}^b-\tau_{31}^a)^2+(\tau_{32}^b-\tau_{32}^a)^2+(v^b-v^a)^2)\,dx\,dy = 0,$$

which is the desired uniqueness result.

4. A signalling problem. In this section we consider an elementary one-dimensional signalling problem for the normalized system (2.48)–(2.53). The solution is of the form

(4.1) $$(\tau_{31},\tau_{32},v) = (\tau(x,t),0,v(x,t)), \qquad 0<x<\infty,$$

where τ and v satisfy

(4.2) $$\frac{\partial\tau}{\partial t} - \frac{\partial v}{\partial x} = -\hat{\alpha}\tau, \qquad 0<x<\infty,$$

(4.3) $$\frac{\partial v}{\partial t} - \frac{\partial\tau}{\partial x} = 0, \qquad 0<x<\infty,$$

and

(4.4) $$\hat{\alpha} = \begin{cases} 1 & \text{if } \tau^2>\tau_y^2, \\ 1 & \text{if } \tau^2=\tau_y^2 \text{ and } \frac{\tau}{\tau_y^2}\frac{\partial v}{\partial x}>1, \\ \frac{\tau}{\tau_y^2}\frac{\partial v}{\partial x}, & \text{if } \tau^2=\tau_y^2 \text{ and } 0\leq\frac{\tau}{\tau_y^2}\frac{\partial v}{\partial x}\leq 1, \\ 0 & \text{if } \tau^2=\tau_y^2 \text{ and } \frac{\tau}{\tau_y^2}\frac{\partial v}{\partial x}<0, \\ 0 & \text{if } \tau^2<\tau_y^2, \end{cases}$$

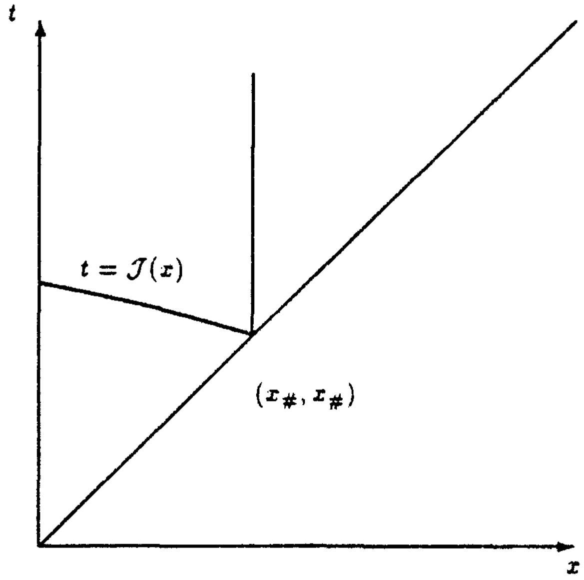

FIG. 1.

and the initial and boundary conditions

$$(\tau, v)(x, 0) = (0, 0), \qquad 0 < x < \infty \tag{4.5}$$

and

$$v(0, t) = -\tau_0, \quad \text{where } \tau_0 > \tau_y. \tag{4.6}$$

We note that the results of the previous section guarantee there is at most one solution to the above problem.

In the region $0 \le t < x$, we have $(\tau, v) \equiv (0, 0)$. Moreover, $\tau + v$ is continuous across the curve $t = x$ and thus satisfies $\tau_-(t, t) + v_-(t, t) \equiv 0$. The difficult part of the problem is to show there is a curve $t = \mathcal{J}(x)$, $0 < x < x_\#$, with $-1 < d\mathcal{J}/dx \le 0$, such that in the region $x < t < \mathcal{J}(x)$ with $0 < x < x_\#$, τ and v satisfy

$$\tau > \tau_y, \tag{4.7}$$

$$\frac{\partial \tau}{\partial t} - \frac{\partial v}{\partial x} = -\tau \quad \text{and} \quad \frac{\partial v}{\partial t} - \frac{\partial \tau}{\partial x} = 0, \tag{4.8}$$

the boundary condition (4.6) and $\tau_-(t, t) + v_-(t, t) = 0$. On the curve $t = \mathcal{J}(x)$ we have $\lim_{\epsilon \to 0^+} \tau(x, \mathcal{J}(x) - \epsilon) = \tau_y$ and $\hat{v}(x) \stackrel{\text{def}}{:=} \lim_{\epsilon \to 0^+} v(x, \mathcal{J}(x) - \epsilon)$ satisfies $0 \le d\hat{v}/dx \le \tau_y$. In the region $\mathcal{J}(x) < t$ and $0 < x < x_\#$ we have $\tau(x, t) = \tau_y$ and $v(x, t) = \hat{v}(x)$, whereas in $x_\# \le x < t$, $\tau \equiv \tau_y$ and $v(x, t) = \hat{v}(x_\#) = -\tau_y$ (see Fig. 1).

The existence of a curve $t = \mathcal{J}(x)$ with the desired properties may be established by converting the system (4.6), (4.8), and $\tau_-(t, t) + v_-(t, t) = 0$ to integral equations for τ and v in $x < t$, verifying that for $0 < t - x \ll 1$ the stress satisfies $\tau > \tau_y$, and finally by obtaining qualitative information on the level line $t = \mathcal{J}(x)$ defined by $\lim_{\epsilon \to 0^+} \tau(x, \mathcal{J}(x) - \epsilon) = \tau_y$.

Rather than perusing that approach we shall show how to obtain simple approximate solutions satisfying (4.6)–(4.8) and $\tau_-(t,t) + v_-(t,t) = 0$ as well as approximations to the level line $t = \mathcal{J}(x)$.

We note that for each integer $N \geq 1$ the system (4.8) has solutions

(4.9) $$v_N = -\tau_0 + \sum_{k=1}^{N} \lambda_{(k)}(t) x^{2k-1}$$

and

(4.10)[6] $$\tau_N = \frac{\lambda_0(t) + \sum_{k=1}^{N} \dot{\lambda}_{(k)} x^{2k}}{2k}$$

$\tau^{2k}/2k$

where the coefficients satisfy

(4.11) $$\dot{\lambda}_0 + \lambda_0 = \lambda_1,$$

(4.12) $$\ddot{\lambda}_k + \dot{\lambda}_k = 2k(2k+1)\lambda_{k+1}, \qquad 1 \leq k \leq N-1,$$

and

(4.13) $$\ddot{\lambda}_N + \dot{\lambda}_N = 0.$$

These solutions satisfy the boundary condition $v_N(0^+,t) = -\tau_0$ and have $2N+1$ free parameters which are determined by insisting that the equation

(4.14) $$\tau_N(t,t) + v_N(t,t) = 0$$

is satisfied to $O(t^{2N})$ as $t \to 0^+$. The approximate curve $t = \mathcal{J}_N(x)$ is subsequently determined by solving $\tau_N(x, \mathcal{J}_N(x)) = \tau_y$. An easy calculation shows that $\mathcal{J}_N(x) = O((\tau_0 - \tau_y)/\tau_0)$ and $d\mathcal{J}_N/dx < 0$ which guarantees that the number $x_\#^N$ defined by $\mathcal{J}_N(x_\#^N) = x_\#^N$ is $O((\tau_0 - \tau_y)/\tau_0)$, and thus on the boundary $x = t$, $\tau_N(t,t) + v_N(t,t)$ is at worst $O((\tau_0 - \tau_y)/\tau_0)^{2N+1}$ for $0 \leq t \leq x_\#^N$. We continue the approximate solutions to the rest of the region described by Fig. 1 via the extensions procedure used for the exact solution; that is, for $0 < t < x$,

(4.15) $$(\tau_N, v_N) \equiv (0,0)$$

for $\mathcal{J}_N(x) < t$ and $0 < x < x_\#^N$

(4.16) $$v_N(x,t) = v_N(x, \mathcal{J}_N(x)) \quad \text{and} \quad \tau_N(x,t) = \tau_y,$$

and for $x_\# \leq x < t$,

(4.17) $$v_N(x,t) = v_N(x_\#, \mathcal{J}_N(x_\#)) \quad \text{and} \quad \tau_N(x,t) = \tau_y.$$

We are then guaranteed that the error made in failing to meet the boundary condition $\tau_N(t,t) + v_N(t,t) = 0$ is at worst $O((\tau_0 - \tau_y)/\tau_0)^{2N+1}$ for all $t > 0$. We shall present the details of this procedure for the case $N = 1$.

In this case,

(4.18) $$v_1 = -\tau_0 + (\lambda_{1,0} + \lambda_{1,1}e^{-t})x$$

[6] Here · denotes differentiation with respect to t.

and

$$\tau_1 = (\lambda_{1,0} + \lambda_{1,1} t e^{-t} + \lambda_{0,1} e^{-t}) - \frac{\lambda_{1,1} e^{-t} x^2}{2}, \tag{4.19}$$

and the insistence that $\tau_1(t,t) + v_1(t,t) = O(t^3)$ as $t \to 0^+$ implies that

$$\begin{aligned} \lambda_{1,0} + \lambda_{0,1} &= \tau_0 \\ \lambda_{1,0} - \lambda_{0,1} + 2\lambda_{1,1} &= 0 \\ \lambda_{0,1} - 5\lambda_{1,1} &= 0 \end{aligned} \tag{4.20}$$

and hence that

$$v_1 = \tau_0 \left(-1 + \frac{(3 + 5e^{-t})x}{8} \right) \tag{4.21}$$

and

$$\tau_1 = \frac{\tau_0}{8} \left(3 + t e^{-t} + 5 e^{-t} - \frac{e^{-t} x^2}{2} \right). \tag{4.22}$$

The approximate curve $t = \mathcal{J}_1(x)$ is obtained by solving $\tau_1(x, \mathcal{J}_1(x)) = \tau_y$ or equivalently the equation

$$\left(3 + \mathcal{J}_1 e^{-\mathcal{J}_1} + 5 e^{-\mathcal{J}_1} - \frac{x^2 e^{-\mathcal{J}_1}}{2} \right) = \frac{8\tau_y}{\tau_0}. \tag{4.23}$$

The fact that $0 < \tau_y/\tau_0 < 1$ guarantees the unique solvability of this equation for $0 \le x \ll 1$ and that $\mathcal{J}_1(0) = O(2((\tau_0 - \tau_y)/\tau_0))$. A quick calculation also shows that

$$\frac{d\mathcal{J}_1}{dx} = \frac{-2x}{(8 + 2\mathcal{J}_1 - x^2)} < 0. \tag{4.24}$$

The number $x_{\#}^1$, where $\mathcal{J}_1(x_{\#}^1) = x_{\#}^1$ satisfies

$$\left(3 + x_{\#}^1 e^{-x_{\#}^1} + 5 e^{-x_{\#}^1} - \frac{(x_{\#}^1)^2 e^{-x_{\#}^1}}{2} \right) = \frac{8\tau_y}{\tau_0}, \tag{4.25}$$

and for $0 < \tau_0 - \tau_y$ small enough we are guaranteed that $x_{\#}^1 = O((\tau_0 - \tau_y)/\tau_0)$. This estimate, when combined with (4.24), implies that $-1 < d\mathcal{J}_1/dx$ for $0 \le x \le x_{\#}^1$.

Our final task is to show that the function

$$\hat{v}_1(x) \stackrel{\text{def}}{:=} \tau_0 \left(-1 + \frac{(3 + 5e^{-\mathcal{J}_1(x)})x}{8} \right) \tag{4.26}$$

satisfies

$$0 \le \frac{d\hat{v}_1}{dx}(x) \le \tau_y, \qquad 0 \le x \le x_{\#}^1. \tag{4.27}$$

The defining relation (4.26) implies that

$$\frac{d\hat{v}_1}{dx}(x) = \tau_0 \left(\frac{3 + 5e^{-\mathcal{J}_1(x)}}{8} \right) - \frac{5\tau_0 e^{-\mathcal{J}_1(x)}}{8} x \mathcal{J}_1'(x), \tag{4.28}$$

and this relationship, when combined with (4.23) and (4.24), implies that

$$\frac{d\hat{v}_1}{dx}(x) = \tau_y + \frac{\tau_0 e^{-\mathcal{J}_1}((x^2 - 2\mathcal{J}_1)(8 + 2\mathcal{J}_1 - x^2) + 20x^4)}{16(8 + 2\mathcal{J}_1 - x^2)}. \tag{4.29}$$

The fact that $\mathcal{J}_1(x) \geq x^1_{\#}$ for $0 \leq x \leq x^1_{\#} = O((\tau_0 - \tau_y)/\tau_0)$ implies that the second term in (4.29) is negative and this provides the desired upper bound for $d\hat{v}_1/dx$. The desired lower bound is an immediate consequence of (4.28) and the bounds for $d\mathcal{J}_1/dx$.

We conclude this section by contrasting the above solution with what obtains if we replace our flow rule—α given by (4.4)—with the one generated by (2.31) and (2.32) and also by the flow rule associated with a rate independent elastic-perfectly plastic material. In the former case, (4.2) is replaced by

$$\frac{\partial \tau}{\partial t} - \frac{\partial v}{\partial x} = -\alpha\tau_y, \tag{4.30}$$

and (4.4) is unchanged.

In the region $0 \leq t < x$ we have $(\tau, v) \equiv (0,0)$, and $\tau + v$ is continuous across $x = t$. For $0 \leq x \leq t \leq 2(\tau_0 - \tau_y)/\tau_y$ we have

$$v = -\tau_0 + \frac{\tau_y x}{2} \quad \text{and} \quad \tau = \tau_0 - \frac{\tau_y t}{2}; \tag{4.31}$$

for $0 \leq x \leq 2(\tau_0 - \tau_y)/\tau_y$ and $t \geq 2(\tau_0 - \tau_y)/\tau_y$ we have

$$v = -\tau_0 + \frac{\tau_y x}{2} \quad \text{and} \quad \tau = \tau_y, \tag{4.32}$$

and finally for $2(\tau_0 - \tau_y)/\tau_y \leq x < t$ we have

$$v = -\tau_y \quad \text{and} \quad \tau = \tau_y. \tag{4.33}$$

With this flow rule the curve $t = \mathcal{J}(\cdot)$ is the constant function $\mathcal{J}(x) = 2(\tau_0 - \tau_y)/\tau_y$, $0 \leq x \leq 2(\tau_0 - \tau_y)/\tau_y$. Equations (2.52) and (2.53), the initial conditions $(F_{31}, p_{31})(x,0) = (0,0)$ for $x > 0$, and (4.31)–(4.33) allow us to determine (F_{31}, p_{31}). The result is

$$(4.34)\quad (F_{31}, p_{31}) = \begin{cases} (0,0), & 0 \leq t < x, \\ (\tau_0 + \tau_y(\frac{t}{2} - x), \tau_y(t - x)), & 0 \leq x < t < \frac{2(\tau_0 - \tau_y)}{\tau_y}, \\ (\tau_0 + \tau_y(\frac{t}{2} - x), \tau_{01} - \tau_y + \tau_y(\frac{t}{2} - x)), & \frac{2(\tau_0 - \tau_y)}{\tau_y} \leq t \quad \text{and} \\ 0 \leq x < \frac{2(\tau_0 - \tau_y)}{\tau_y}, & \\ (\tau_y, 0), & \frac{2(\tau_0 - \tau_y)}{\tau_y} < x < t. \end{cases}$$

It is worth noting that the above solution is unique. This can be established using the arguments of §3 directly on the system (4.30) and (4.3)–(4.6).

We now examine the signaling problem for a rate independent elastic-perfectly plastic material. Equations (4.1)–(4.3) and (4.5) and (4.6) still hold, except now $\hat{\alpha}$ is given by

$$\hat{\alpha} = \begin{cases} 0 & \text{if } \tau^2 < \tau_y^2 \\ 0 & \text{if } \tau^2 = \tau_y^2 \quad \text{and} \quad \frac{\tau}{\tau_y^2}\frac{\partial v}{\partial x} < 0, \\ \frac{\tau}{\tau_y^2}\frac{\partial v}{\partial x} & \text{if } \tau^2 = \tau_y^2 \quad \text{and} \quad 0 \leq \frac{\tau}{\tau_y^2}\frac{\partial v}{\partial x}. \end{cases} \tag{4.35}$$

We also have

$$\frac{\partial F_{31}}{\partial t} - \frac{\partial v}{\partial x} = 0, \quad \frac{\partial p_{31}}{\partial t} = \hat{\alpha}\tau, \quad \text{and} \quad F_{31} = \tau + p_{31}, \tag{4.36}$$

and these satisfy the initial conditions

$$(F_{31}, p_{31})(x, 0) = (0, 0), x > 0. \tag{4.37}$$

We seek solutions with structure similar to that obtained for the previous two models. Specifically, a shock curve $t = \hat{t}(x)$ such that in the region $0 < t < \hat{t}(x)$,

$$(F_{31}, p_{31}, \tau, v) = (0, 0, 0, 0), \tag{4.38}$$

and in the region $t > \hat{t}(x)$ the shear stress τ is at yield, i.e.,

$$\tau(x, t) = \tau_y, \qquad \hat{t}(x) < t. \tag{4.39}$$

We interpret (4.3) and (4.36) as conservation laws, and this, together with (4.38) and (4.39), implies that on $t = \hat{t}(x)$,

$$v^-(x, \hat{t}(x)) + \tau_y \frac{d\hat{t}}{dx} = 0 \tag{4.40}$$

and

$$F_{31}^-(x, \hat{t}(x)) + v^-(x, \hat{t}(x)) \frac{d\hat{t}}{dx} = 0. \tag{4.41}$$

Here, $(v^-, F_{31}^-)(x, \hat{t}(x)) = \lim_{\epsilon \to 0^+}(v, F_{31})(x - \epsilon, \hat{t}(x))$. The identity (4.39) also implies that in $t > \hat{t}(x)$ the velocity v is a function of x only. Near $x = 0$ we choose

$$v(x, t) = -\tau_0 + \lambda x, \lambda > 0. \tag{4.42}$$

With this choice we obtain

$$p_{31} = \lambda(t - \hat{t}(x)) + p_-(x) \tag{4.43}$$

and

$$F_{31} = \tau_y + \lambda(t - \hat{t}(x)) + p_-(x). \tag{4.44}$$

Equation (4.40), together with $\hat{t}(0) = 0$, then yields

$$\hat{t}(x) = \frac{\tau_0^2 - (\tau_0 - \lambda x)^2}{2\lambda\tau_y}, \tag{4.45}$$

and (4.41),(4.44), and (4.45) imply that

$$p_-(x) = \frac{(\tau_0 - \lambda x^2) - \tau_y^2}{\tau_y}. \tag{4.46}$$

We now let

$$x_\# = \frac{\tau_0 - \tau_y}{\lambda} \tag{4.47}$$

and note that

$$p_-(x) > 0, \qquad 0 \le x < x_\#, \tag{4.48}$$

$$p_-(x_\#) = 0, \tag{4.49}$$

and

$$\frac{d\hat{t}}{dx}(x_\#) = 1. \tag{4.50}$$

In the region $(\tau_0^2 - (\tau_0 - \lambda x)^2)/2\lambda\tau_y < t$ and $0 \le x < x_\# = (\tau_0 - \tau_y)/\lambda$ our solution is given by

$$F_{31} = \tau_y + \lambda\left(t + \frac{\tau_0^2 - (\tau_0 - \lambda x)^2}{2\lambda\tau_y}\right), \tag{4.51}$$

$$p_{31} = \lambda\left(t + \frac{\tau_0^2 - (\tau_0 - \lambda x)^2}{2\lambda\tau_y}\right), \tag{4.52}$$

$$v = -\tau_0 + \lambda x, \tag{4.53}$$

$$\tau = \tau_y. \tag{4.54}$$

The shock curve is continued to $x > x_\#$ by

$$\hat{t}(x) = \frac{\tau_0^2 - \tau_y^2}{2\lambda\tau_y} + \left(x - \frac{\tau_0 - \tau_y}{\lambda}\right) \tag{4.55}$$

and in the region $((\tau_0^2 - \tau_y^2)/2\lambda\tau_y) + (x - ((\tau_0 - \tau_y)/\lambda)) < t$ and $(\tau_0 - \tau_y)/\lambda = x_\# < x$,

$$F_{31} = \tau_y, \quad p_{31} = 0, \quad v = -\tau_y, \quad \text{and} \tau = \tau_y. \tag{4.56}$$

The line $x = x_\# = (\tau_0 - \tau_y)/\lambda$ is a stationary contact discontinuity and across it p_{31} jumps while the other fields are continuous. The interesting fact about the signaling problem for this model is the lack of unicity of solutions; we have a compatible solution for every $\lambda > 0$. This observation points out one of the weaknesses of the classical model.

5. Computational experiments. In this section we present the results of a computational experiment performed on the normalized system (2.48)–(2.52) when the pressure gradient is zero. The results reported deal with a two-dimensional generalization of the signalling problem of the previous section.

The experiment deals with the system (2.48)–(2.51) solved in the region $r > 0$ and $\pi/2 < \theta < 2\pi$, where $r = \sqrt{x^2 + y^2}$. At time $t = 0$ we assume that

$$(\tau_{31}, \tau_{32}, v) = (0, 0, 0) \tag{5.1}$$

for $r > 0$ and $\pi/2 < \theta < 2\pi$, and for $t > 0$ we assume that

$$v\left(r, \frac{\pi}{2}^+\right) = v(r, 2\pi^-) = \tau_0, \qquad r > 0, \tag{5.2}$$

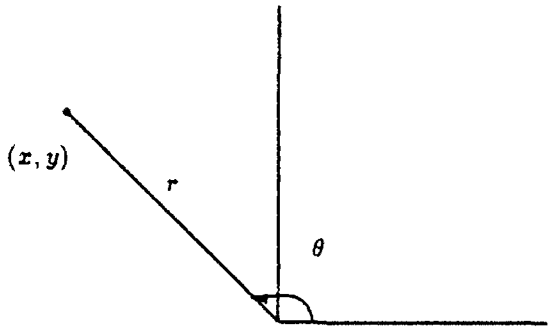

FIG. 2.

where $\tau_0 > \tau_y$, and again $\tau_y > 0$ is the yield stress.

The elastic version of this problem, namely, the system

$$\frac{\partial \tau_{31}}{\partial t} - \frac{\partial v}{\partial x} = 0, \tag{5.3}$$

$$\frac{\partial \tau_{32}}{\partial t} - \frac{\partial v}{\partial y} = 0, \tag{5.4}$$

$$\frac{\partial v}{\partial t} - \frac{\partial \tau_{31}}{\partial x} - \frac{\partial \tau_{32}}{\partial y} = 0, \tag{5.5}$$

together with (5.1) and (5.2), was considered by Keller and Blank [13]. They obtained exact solutions to this and a number of other problems with self similar structure. Relevant to us here is the singular nature of $\tau_{31}^2 + \tau_{32}^2$ as $r \to 0^+$. Their results demonstrate that

$$\tau_{31}^2 + \tau_{32}^2 = O\left(\frac{t}{r}\right)^{2/3}, \qquad r \to 0^+. \tag{5.6}$$

This singular behavior also obtains for the plastic flow problem and forces us to treat the boundary conditions in our numerical simulation carefully. Our integration scheme for (2.48)–(2.51) is based on a symmetrized operator splitting algorithm for the governing differential equations. At time $t = nh$, $n = 0, 1, 2, \ldots$, our approximate solution consists of lattice data

$$(\tau_{31}, \tau_{32}, v)^n_{(k,m)} = (\tau_{31}, \tau_{32}, v)\left(\frac{(2k-1)}{2}h, \frac{(2m-1)}{2}h, nh\right). \tag{5.7}$$

For the problem under consideration the boundaries are not part of the computational lattice but are offset from it by a distance of $h/2$. The computational lattice is

$$\mathcal{S} = \{(k,m) \mid k \le 0 \text{ and } m = 0, \pm 1, \pm 2, \ldots\} \cup \{(k,m) \mid k \ge 1 \text{ and } m \le 0\}. \tag{5.8}$$

To update the data (5.7) we successively solve

$$\frac{\partial \tau_{31}}{\partial t} - \frac{\partial v}{\partial x} = 0, \quad \frac{\partial \tau_{32}}{\partial t} = 0, \quad \text{and} \quad \frac{\partial v}{\partial t} - \frac{\partial \tau_{31}}{\partial x} = 0, \quad 0 \le t \le h, \tag{5.9}$$

$$\frac{\partial \tau_{31}}{\partial t} = 0, \quad \frac{\partial \tau_{32}}{\partial t} - \frac{\partial v}{\partial y} = 0, \quad \text{and} \quad \frac{\partial v}{\partial t} - \frac{\partial \tau_{32}}{\partial y} = 0, \quad 0 \le t \le h, \tag{5.10}$$

and

$$\frac{\partial \tau_{31}}{\partial t} = -\hat{\alpha}\tau_{31}, \quad \frac{\partial \tau_{32}}{\partial t} = -\hat{\alpha}\tau_{32}, \quad \text{and} \quad \frac{\partial v}{\partial t} = 0, \quad 0 \le t \le h, \tag{5.11}$$

where of course $\hat{\alpha}$ is defined in (2.51). For (5.9) we use the approximate solution defined by (5.7) as initial data and let $(\tau_{31}^1, \tau_{32}^1, v^1)_{(k,m)}$ denote the value of this solution at $t = h$ on the lattice $\mathcal{S}$. We then solve (5.10) using the $(\tau_{31}^1, \tau_{32}^1, v^1)_{(k,m)}$ as initial data and let $(\tau_{31}^2, \tau_{32}^2, v^2)_{(k,m)}$ denote value of the solution at $t = h$ on $\mathcal{S}$. Finally, we solve (5.11) with $(\tau_{31}^2, \tau_{32}^2, v^2)_{(k,m)}$ as initial data and let $(\tau_{31}^3, \tau_{32}^3, v^3)_{(k,m)}$ denote the value of this solution at $t = h$ on $\mathcal{S}$.

We then repeat the process solving (5.10) first with the data (5.7), and, we let $(\tau_{31}^4, \tau_{32}^4, v^4)_{(k,m)}$ denote the lattice update at $t = h$. We then solve (5.9) using $(\tau_{31}^4, \tau_{32}^4, v^4)_{(k,m)}$ as initial data and let $(\tau_{31}^5, \tau_{32}^5, v^5)_{(k,m)}$ denote the lattice update. Finally we solve (5.11) with data $(\tau_{31}^5, \tau_{32}^5, v^5)_{(k,m)}$ and let $(\tau_{31}^6, \tau_{32}^6, v^6)_{(k,m)}$ denote the lattice update at $t = h$. The desired approximate solution $(\tau_{31}, \tau_{32}, v)_{(k,m)}^{(n+1)}$ is then obtained by averaging $(\tau_{31}^3, \tau_{32}^3, v^3)_{(k,m)}$ and $(\tau_{31}^6, \tau_{32}^6, v^6)_{(k,m)}$; that is,

insert one sees not only

$$(\tau_{31}, \tau_{32}, v)_{(k,m)}^{(n+1)} = \tfrac{1}{2}(\tau_{31}^3 + \tau_{31}^6, \tau_{32}^3 + \tau_{32}^6, v^3 + v^6)_{(k,m)}. \tag{5.12}$$

Of course, all of the intermediate updates are solved subject to the boundary conditions of the original problem. Here these boundary conditions manifest themselves as reflection conditions at those lattice points that are a distance $h/2$ away form the actual boundary. Formal accuracy could be maintained if we used either $(\tau_{31}^3, \tau_{32}^3, v^3)_{(k,m)}$ or $(\tau_{31}^6, \tau_{32}^6, v^6)_{(k,m)}$ for the updated approximate solution but either of these updates alone would, over time, tend to introduce asymmetries into the approximates not present in the actual solution. These asymmetries are removed with the algorithm employed.

The results of our experiment are shown in Figs. 3–7. Each snapshot shows two different representations of the velocity field and the total shear stress, namely the quantity $\sqrt{\tau_{31}^2 + \tau_{32}^2}$. This simulation was run with $h = 1/50$, $\tau_y = 1$, and $\tau_0 = 1.3$. The contours on the velocity plots are spaced 0.1 apart and run from $v = 0$ to $v = 1.3$. The stress contours run from 1 to 3.2 in increments of 0.2. In these snapshots ~~we do not see any of~~ the plane wave solutions of the previous section but also the effect of the corner singularity which are confined to the region $0 \le r \le t$ and $\pi/2 < \theta < 2\pi$.

For comparison we have run the elastic version of this problem with the same boundary conditions and same values of h, τ_y, and τ_0. These results are shown in

delete Figs. 8–12. delete

It should be noted that for both problems the velocity fields satisfy the additional condition

$$\lim_{r \to t^{+}} v(r, \theta, t) = 0, \qquad \frac{\pi}{2} < \theta < 2\pi \tag{5.13}$$

$r \to t^+$

and that our numerical solutions meet this consistency condition automatically.

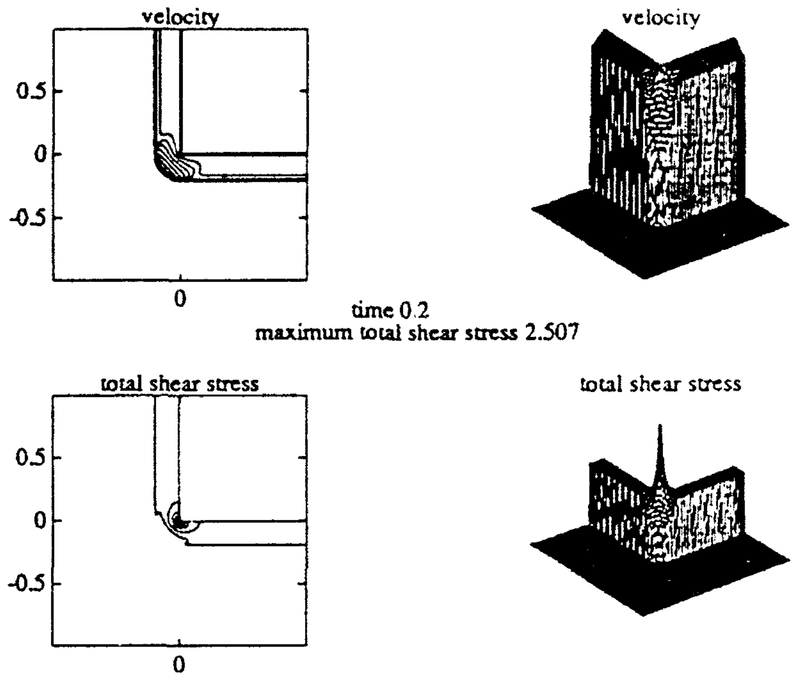
velocity
0.5
0
-0.5
0
velocity
time 0.2
maximum total shear stress 2.507
total shear stress
0.5
0
-0.5
0
total shear stress

Fig. 3

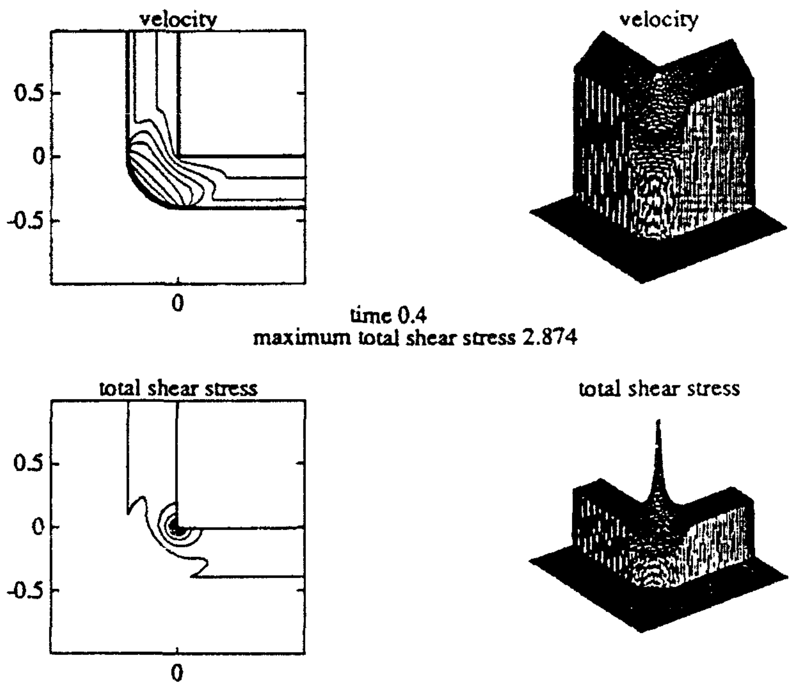
velocity
0.5
0
-0.5
0
velocity
time 0.4
maximum total shear stress 2.874
total shear stress
0.5
0
-0.5
0
total shear stress

Fig. 4

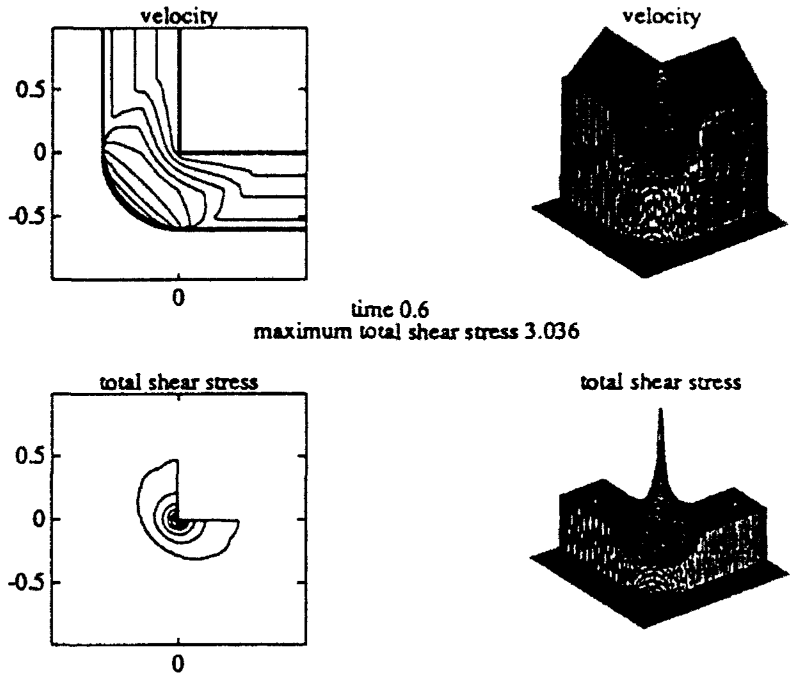
velocity
velocity
0.5
0
-0.5
0
time 0.6
maximum total shear stress 3.036
total shear stress
total shear stress
0.5
0
-0.5
0

Fig. 5

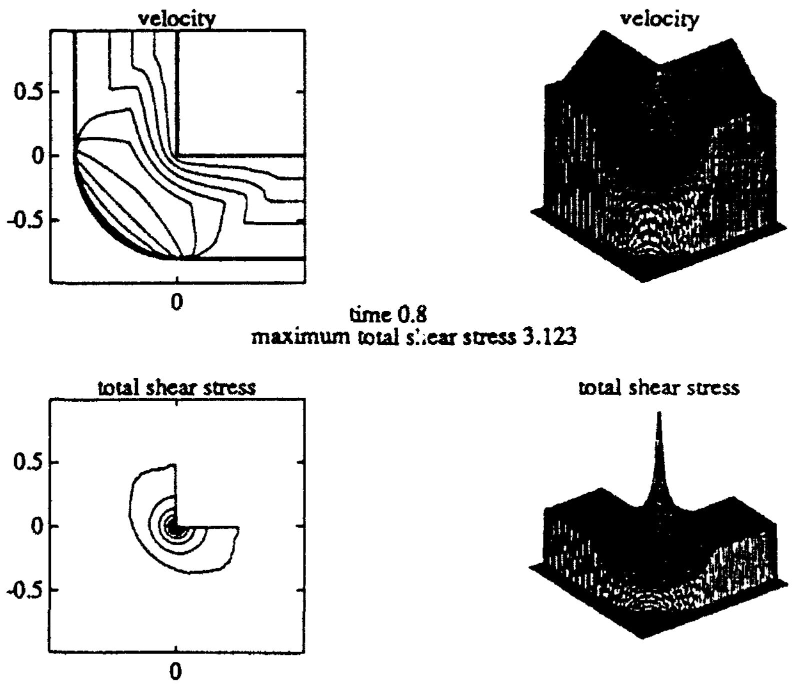
velocity
velocity
0.5
0
-0.5
0
time 0.8
maximum total shear stress 3.123
total shear stress
total shear stress
0.5
0
-0.5
0

Fig. 6

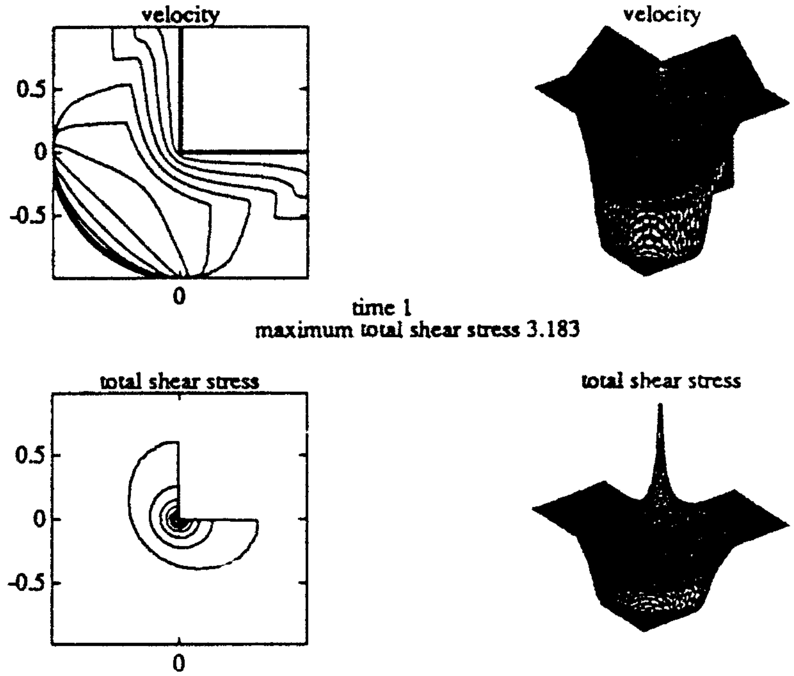
velocity
velocity
0.5
0
-0.5
0
time 1
maximum total shear stress 3.183
total shear stress
total shear stress
0.5
0
-0.5
0

Fig. 7

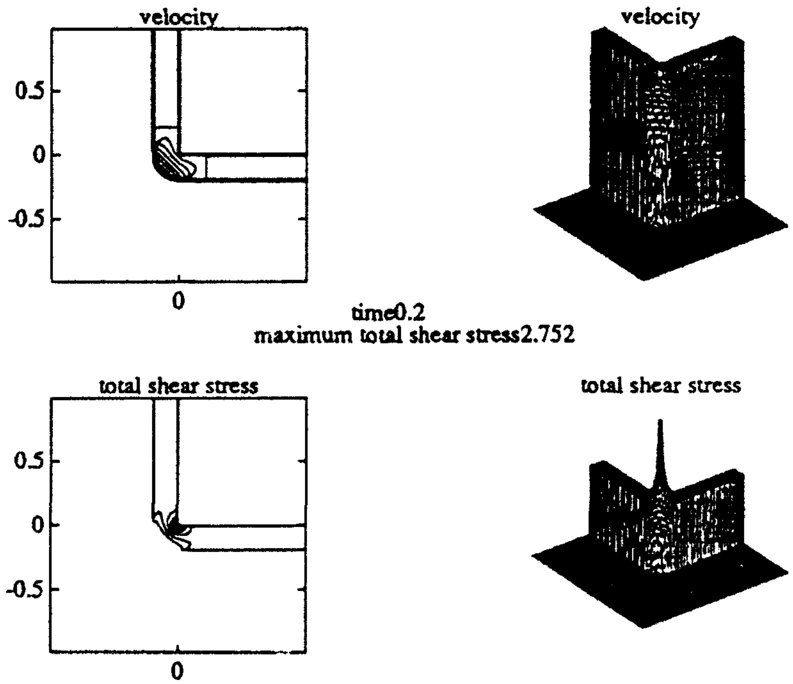
velocity
velocity
0.5
0
-0.5
0
time0.2
maximum total shear stress2.752
total shear stress
total shear stress
0.5
0
-0.5
0

Fig. 8

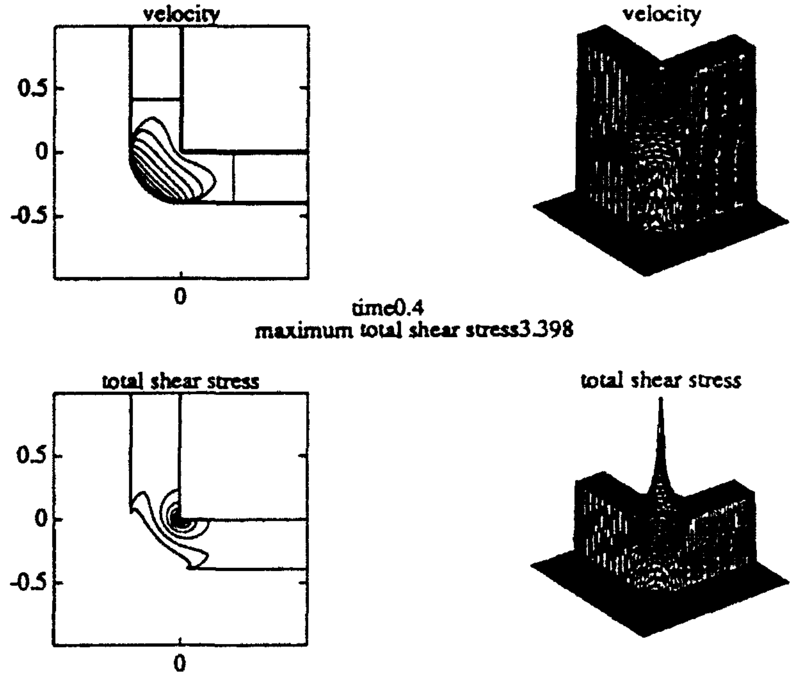
velocity
velocity
0.5
0
-0.5
0
time0.4
maximum total shear stress3.398
total shear stress
total shear stress
0.5
0
-0.5
0

Fig. 9

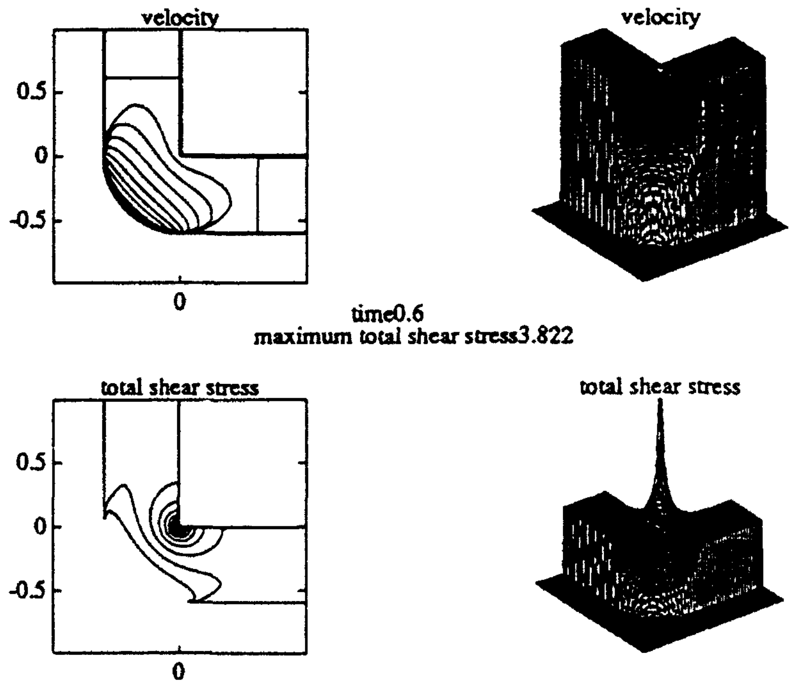
velocity
velocity
0.5
0
-0.5
0
time0.6
maximum total shear stress3.822
total shear stress
total shear stress
0.5
0
-0.5
0

Fig. 10

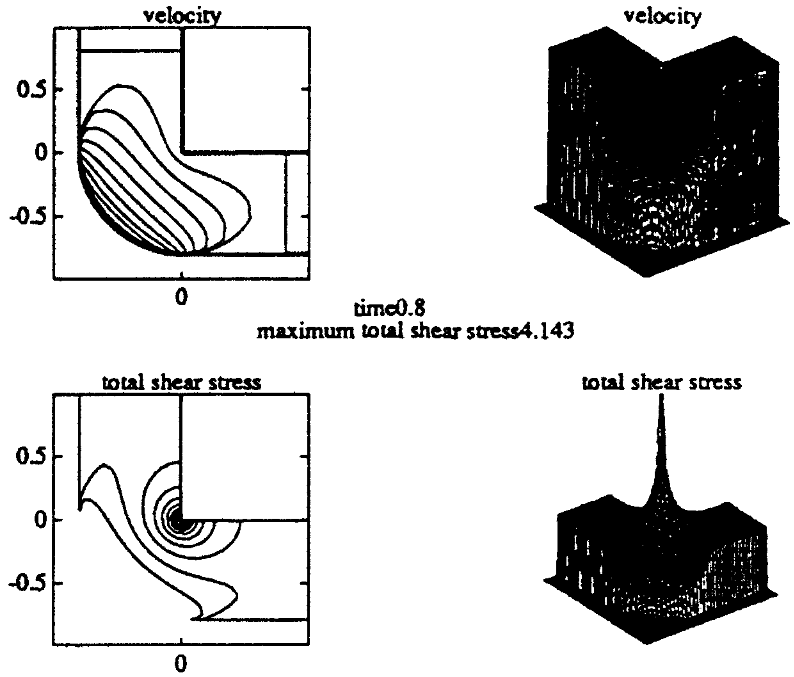
velocity
velocity
0.5
0
-0.5
0
time0.8
maximum total shear stress4.143
total shear stress
total shear stress
0.5
0
-0.5
0

Fig. 11

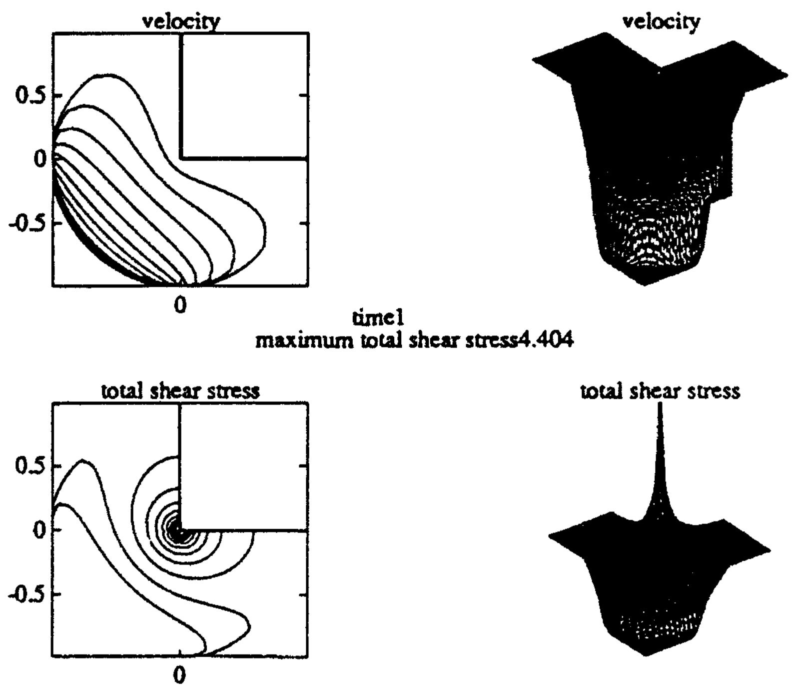
velocity
velocity
0.5
0
-0.5
0
time1
maximum total shear stress4.404
total shear stress
total shear stress
0.5
0
-0.5
0

Fig. 12

REFERENCES

[1] J. M. GREENBERG, *Models of elastic-perfect plastic materials*, Euro. J. Appl. Math. 1 (1990), pp. 131–150.

[2] ———, ~~*The longtime behavior of elastic-perfectly plastic materials*, Proceedings of the Fifth International Conference on Free Boundary Problems, to appear, 1990.~~

[3] T. I. SEIDMAN, *Event-driven discontinuities for continuous-time systems*, in Proc. 28th IEEE Conf. Decision and Control, (1989), pp. 795–796.

[4] V. I. UTKIN, *Sliding models and their application in variable structure systems*, Mir, Moscow, 1978.

[5] A. F. FILIPPOV, *Differential equations with discontinuous righthand sides*, Kluwer, Dordrecht, 1978.

[6] S. S. ANTMAN AND W. G. SZYMCZAK, *Nonlinear elastoplastic wave*, Contemp. Math., 100 (1989), pp. 27–54.

[7] ———, *Large antiplane shearing motion of nonlinear viscoplastic materials*, preprint, 1990.

[8] B. D. COLEMAN AND D. R. OWEN, *On Thermodynamics and Elastic-Plastic Materials*, Arch. Rational Mech. Anal., 59 (1975), pp. 25–51.

[9] J. L. BUHITE AND D. R. OWEN, *An Ordinary Differential Equation From the Theory of Plasticity*, Arch. Rat Mech. Anal., 71 (1979), pp. 357–383.

[10] B. D. COLEMAN AND M. L. HODGDON, *On Shear Bands in Ductile Materials*, Arch. Rational Mech. Anal., 90 (1985), pp. 219–247.

[11] D. R. OWEN, *Weakly decaying energy separation and uniqueness of motions of an elastic-plastic oscillator with work-hardening*, Arch. Rational Mech. Anal. 98 (1979), pp. 95–114.

[12] M. E. GURTIN, *Topics in Finite Elasticity*, CBMS-NSF Regional Conference Series in Applied Mathematics, Society for Industrial and Applied Mathematics, Philadelphia, PA, 1980.

[13] J. B. KELLER AND A. BLANK, *Diffraction and reflection of pulses by wedges and corners*, Comm. Pure and Appl. Math., 4 (1957), pp. 75–91.

— The long time behavior of elastic-perfectly plastic materials, in Free boundary problems involving solids – Proceedings of the International Colloquium 'Free Boundary Problems: Theory and Applications', ed J. M. Chadam an H. K. Rasmussen, Longman Scientific and Technical (1993), pp 28-34.